의학박사 학위논문

Analysis on swallowing kinematic features in patients with stroke & Parkinson's disease and development of prognostic models for post-stroke dysphagia

뇌졸중과 파킨슨병 환자의 삼킴에 대한 운동학적 특징 분석 및 뇌졸중 후 삼킴곤란의 예후 예측 모델 개발

2020년 2월

서울대학교 대학원

의학과 의공학 전공

이 우 형

뇌졸중과 파킨슨병 환자의 삼킴에 대한 운동학적 특징 분석 및 뇌졸중 후 삼킴곤란의 예후 예측 모델 개발

지도교수 김 성 완

이 논문을 의학박사 학위논문으로 제출함

2019년 10월

서울대학교 대학원

의학과 의공학 전공

이 우 형

이우형의 의학박사 학위논문을 인준함

2019년 12월

위원장 _____ (인)

부위원장 _____ (인)

위 원 _____ (인)

위 원 _____ (인)

위 원 _____ (인)

Analysis on swallowing kinematic features in patients with stroke & Parkinson's disease and development of prognostic models for post-stroke dysphagia

By

Woo Hyung Lee

(Directed by Sungwan Kim, PhD)

A thesis submitted to the Department of Medicine in partial fulfilment of the requirements for the Degree of Doctor of Philosophy in Biomedical Engineering at Seoul National University College of Medicine

December 2019

Approved by Thesis Committee:

Professor _____ Chairman
Professor _____ Vice chairman
Professor _____
Professor _____
Professor _____

Abstract

Analysis on swallowing kinematic features in patients with stroke & Parkinson's disease and development of prognostic models for post-stroke dysphagia

Woo Hyung Lee

Department of Biomedical Engineering

Seoul National University College of Medicine

Introduction: Dysphagia is one of the most common symptoms with increasing prevalence in brain disorders. Particular attention necessitates to examine and manage dysphagia since the resultant aspiration pneumonia can be a major cause of death in patients with brain disorders. The aim of the present study was to explore novel kinematic features of swallowing in patients with Parkinson's disease (PD) and stroke and to develop and validate machine learning-based prognostic models to predict functional swallowing status in patients with post-stroke dysphagia.

Methods: Characteristic hyoid kinematics in patients with PD and ischemic stroke were investigated in this study. For ischemic stroke patients, clinical and radiologic factors that are associated with 6-month swallowing recovery were additionally

explored and utilized with kinematic factors to develop prognostic models for prediction of 6-month swallowing recovery. In the kinematic analysis for PD patients and healthy controls, spatiotemporal data of the hyoid bone was obtained from videofluoroscopic swallowing study (VFSS) images of 69 subjects (23 patients with PD, 23 age- and sex-matched healthy elderly controls, and 23 healthy young controls). Normalized profiles of displacement/velocity during swallowing were analyzed using functional regression analysis and their maximal values were compared among the three groups. In the kinematic analysis for patients with ischemic stroke, 18 patients with poor prognosis (no recovery to pre-stroke status at 6 months) and 18 age- and sex-matched patients with good prognosis (recovery to pre-stroke status at 6 months) were selected among the consecutive patients (N=137) with post-stroke dysphagia. Normalized profiles of displacement/velocity and direction angle of the hyoid bone were analyzed using functional regression analysis and their maximal or mean values were compared among the patients with good and poor prognosis. In survival analysis, the Kaplan-Meier method and Cox regression model were used for 137 patients with ischemic stroke to explore clinical and radiologic factors associated with poor prognosis of swallowing function. An extreme gradient boosting (XGBoost) model was developed to classify patients into those with good and poor recovery of swallowing function based on the relevant kinematic, clinical, and radiologic factors. The developed models were verified using 5-fold cross-validation, and the prediction performance was compared with that of other benchmarking classifiers based on support vector machine, random forest, and artificial neural networks.

Results: In the kinematic analysis for PD patients and healthy controls, maximal horizontal displacement and velocity were significantly decreased during the initial

backward (P=0.006 and P<0.001, respectively) and forward (P=0.008 and P<0.001, respectively) motions of the hyoid bone in PD patients compared to elderly controls. Maximal vertical velocity was significantly lower in PD patients than in elderly controls (P=0.001). No significant difference was observed in maximal displacement and velocity in both horizontal and vertical planes between the healthy elderly and young controls. In the kinematic analysis for patients with ischemic stroke, both maximal horizontal displacement (P=0.031) and velocity (P=0.034) in the forward hyoid motions were reduced significantly in patients with poor prognosis compared to those with good prognosis. The mean direction angle for the initial swallowing phase was significantly lower in patients with poor prognosis than those with good prognosis (P=0.050). Survival analysis for patients with post-stroke dysphagia indicated that twenty-four (17.5%) patients showed persistent dysphagia until 6 months after stroke onset with a mean duration of 65.6 days. The time duration of post-stroke dysphagia significantly differed by initial tube feeding, clinical dysphagia scale, sex, severe white matter hyperintensities, and bilateral lesions at the corona radiata, basal ganglia, and/or internal capsule (CR/BG/IC). Among these factors, initial tube feeding (P<0.001), bilateral lesions at CR/BG/IC (P=0.001), and clinical dysphagia scale (P=0.042) were significant prognostic factors in the multivariate analysis using Cox regression models. In prediction of 6-month swallowing recovery, the XGBoost classifier outperforms the benchmarking classifiers based on support vector machine, random forest, and artificial neural networks with an area under the ROC curve of 0.881, F1 score of 0.945, and Matthews correlation coefficient of 0.718.

Conclusions: The present study revealed that altered initial backward motions of the hyoid bone during swallowing can be the novel differential kinematic features in

dysphagia patients with PD and ischemic stroke. In ischemic stroke patients, initial dysphagia severity and bilateral lesions at CR/BG/IC were significant clinical and radiologic factors associated with 6-month swallowing recovery, respectively. Prediction of 6-month swallowing recovery in post-stroke dysphagia was feasible using the proposed XGBoost model based on the kinematic, clinical, and radiologic factors. This study emphasizes that altered initial backward motions of the hyoid bone and bilateral subcortical lesions are important prognostic factors and can be utilized to develop prognostic models for long-term swallowing recovery in ischemic stroke. Future study is warranted to explore physiological aspects of initial hyoid motions and bilateral subcortical lesions on recovery of swallowing function and improve prognostic models for long-term swallowing recovery based on these investigations.

Keywords: Deglutition; Functional data; Hyoid bone; Machine learning; Motion analysis; Parkinson’ s disease; Prognosis; Stroke; Survival analysis

Student Number: 2012-23642

Table of Contents

List of Tables

List of Figures

List of Abbreviations

ASHA NOMS American speech–language–hearing association's national outcome measurement system

AUC Area under the curve

BG Basal ganglia

C2 The second cervical vertebral body

C4 The fourth cervical vertebral body

CDS Clinical dysphagia scale

CR Corona radiata

FLAIR Fluid attenuated inversion recovery

FLR Functional linear regression model

FN False negative

FP False positive

HD Displacement of the hyoid bone

HV Velocity of the hyoid bone

IC Internal capsule

MCC Matthews correlation coefficient

MRI Magnetic resonance imaging

NIHSS National institutes of health stroke scale

PD Parkinson's disease

PENSSE The penalized sum of squares

RMSE Root mean squared error

ROC Receiver operating characteristic

TN True negative

TP True positive

VDS Videofluoroscopic dysphagia scale

VFSS Videofluoroscopy swallowing study

WMH White matter hyperintensities

XGBoost Extreme gradient boosting

1. Introduction

1.1. Dysphagia in Brain Disorders

Dysphagia is one of the most common symptoms with increasing prevalence in brain disorders. The prevalence of dysphagia has been reported as 87% in Parkinson's disease (PD),[1] 65% in acute stroke,[2] 25-61% in traumatic brain injury,[3,4] and 32-84% in Alzheimer's dementia.[5,6] Dysphagia is defined as the difficulty to effectively move the alimentary bolus from the mouth to the esophagus.[7] It can occur by sudden onset neuronal injury or develops insidiously with a slowly progressive disease course in brain disorders. In any clinical courses, particular attention necessitates to detect and manage dysphagia with a caution since the resultant aspiration pneumonia is a major cause of death in patients with brain disorders.[8] The affected patients can also suffer from malnutrition, dehydration, and poor quality of life,[9,10] which leads to increased institutionalization rate after discharge and decreased functional capacity in the long-term period.[11]

In PD patients, swallowing changes can occur insidiously during clinical evolution of the disease.[12] The oropharyngeal musculatures which are involved in the swallowing process can be impaired even in the early-stage PD patients without subjective swallowing difficulty.[13] This can be represented as reduced swallowing speed and decreased motions of lingual and palatal areas.[14] There has been growing evidence of peripheral mechanisms affecting swallowing-associated peripheral nerves and muscles as well as reduced dopaminergic activity in the basal ganglia for the pathophysiology of PD-related dysphagia.[15] Involvement of both central and

peripheral nervous system can cause abnormal recruitment of the muscles during swallowing, which may result in impaired control of the hyoid motions.

Post-stroke dysphagia is also one of the high prevalent complications.[2] Generally, post-stroke dysphagia shows relatively rapid recovery over days to weeks.[9] This clinical course is distinct from other neurodegenerative disorders in which swallowing function deteriorates gradually with disease progression.[16] In neurophysiology, swallowing musculature is asymmetrically represented at bilateral motor cortices of the brain.[17] The asymmetric bilaterality can be one of the plausible hypotheses to lead patients with post-stroke dysphagia to regain swallowing competence over a comparatively short period.[18] Despite the benign clinical course, 13-18% of patients can still suffer from persistent dysphagia until 6 months from stroke onset.[9,19] Moreover, patients with post-stroke dysphagia showed increased rates of pulmonary infection and mortality among stroke survivors by 17% and 30%, respectively.[16] Effort to identify the high risk group of patients with severe dysphagia is needed by exploring the important prognostic factors to be associated with poor recovery of swallowing function. The potential prognostic factors may incorporate various types of patient information based on clinical, radiological, and swallowing kinematic knowledge.

1.2. Swallowing Kinematic Analysis

1.2.1. Kinematic Characteristics of the Hyoid Bone during Swallowing

In swallowing dynamics, hyoid excursion is one of the main physiological events during the pharyngeal phase of swallowing.[20–22] It is an important process to exert thyrohyoid approximation resulting in an epiglottic tilt and actively open the upper esophageal sphincter, leading to protection of the airway from bolus aspiration.[23,24] In normal swallowing, the trajectory pattern of the hyoid bone is significantly influenced by sequential contractions of the hyoid-adjacent muscles including the stylohyoid, posterior digastric, and mylohyoid muscles, followed by the geniohyoid and anterior digastric muscles (Fig. 1.1, Fig. 1.2).[25] Substantial impairment in hyoid excursion induces post-swallow pharyngeal residues and a greater risk of penetration-aspiration (Fig. 1.3).[26] Since the sequence of muscle activity is constant during the pharyngeal phase,[25] any impairment of the hyoid-adjacent muscles disturbing the swallow sequence can influence the trajectory of the hyoid bone and result in swallowing dysfunction.[27]

Previous kinematic studies have shown impaired movements of the hyolaryngeal complex in patients with PD[28,29] or stroke[30]-related dysphagia. These studies ascertained the effects of diseases on the hyoid motions by analyzing only specific variables such as maximum or mean values rather than the entire profile of movements over time. This conventional method might be limited to analyze changes of the hyoid trajectories over time in that hyoid positional data vary during swallowing process, but are not included in the analysis.[31] The methods analyzing

continuous positional variation may necessitate complex analytical algorithms and heavy computation, which has impeded investigations on differential trajectories of the hyoid bone during swallowing in patients with brain disorders.

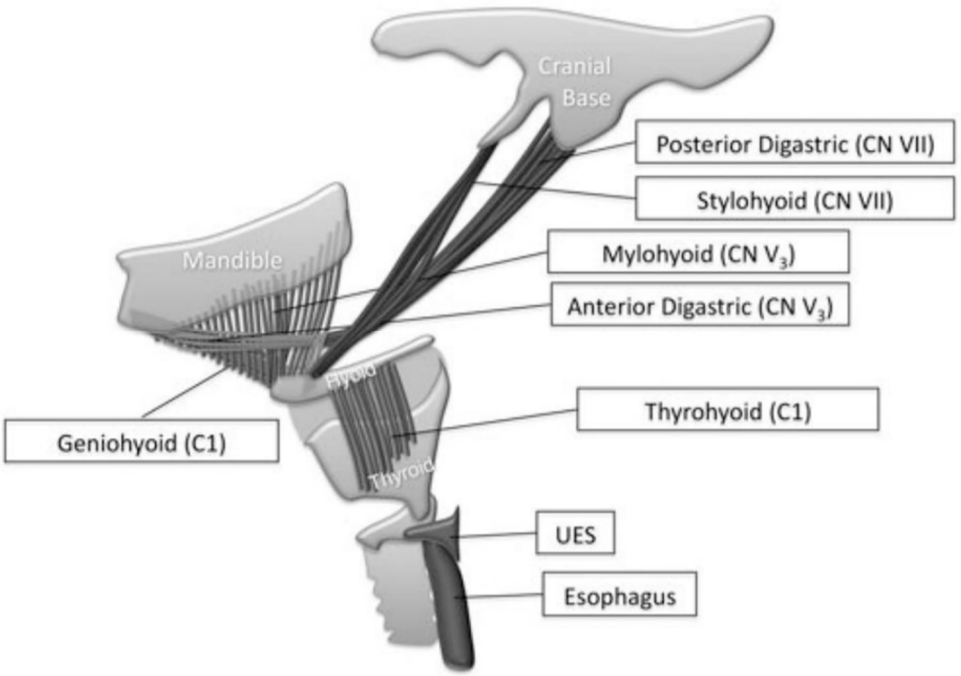

Fig. 1.1. Anatomy of the hyoid bone and adjacent supra- and infrahyoid muscles. Reprinted by permission from "Springer Nature: Dysphagia, vol. 26, Evaluating the Structural Properties of Suprahyoid Muscles and their Potential for Moving the Hyoid, William G. Pearson Jr. et al., p. 345-351, Copyright, 2011".[32]

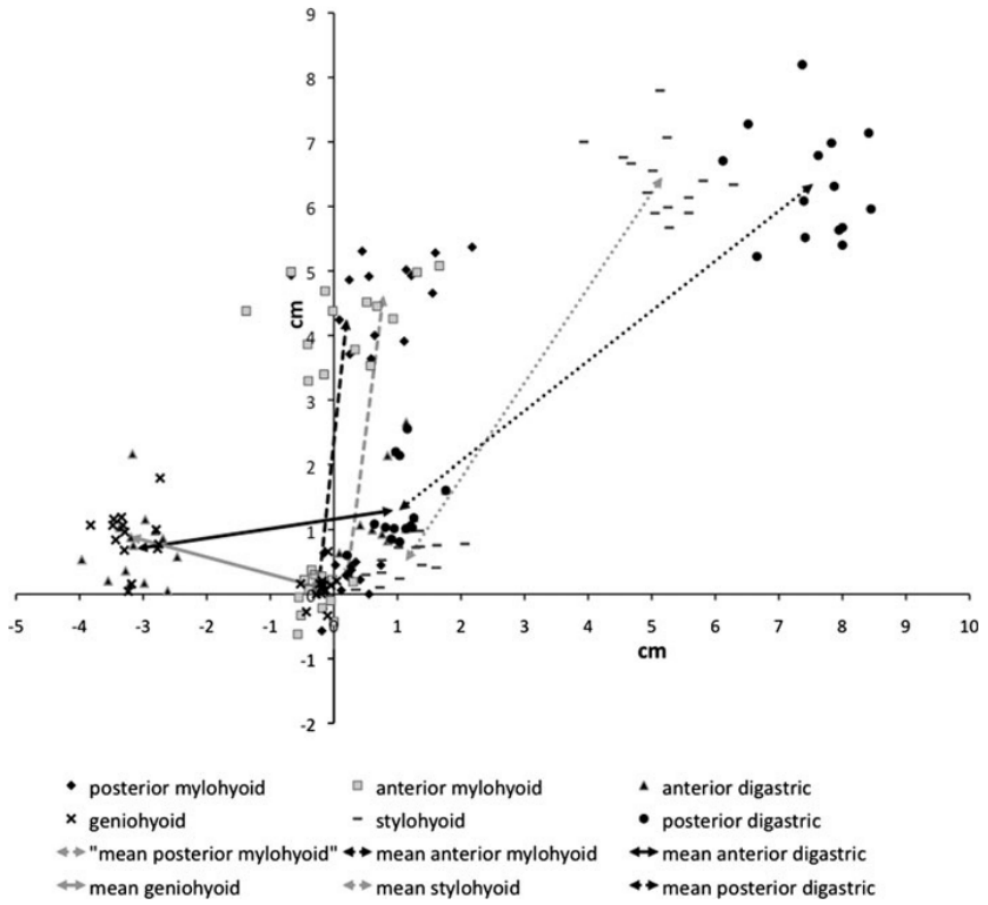

Fig. 1.2. Two-dimensional coordinates of attachment points and action in the supra- and infrahyoid muscles. Arrows indicate a mean line of muscle actions. Reprinted by permission from "Springer Nature: Dysphagia, vol. 26, Evaluating the Structural Properties of Suprahyoid Muscles and their Potential for Moving the Hyoid, William G. Pearson Jr. et al., p. 345-351, Copyright, 2011".[32]

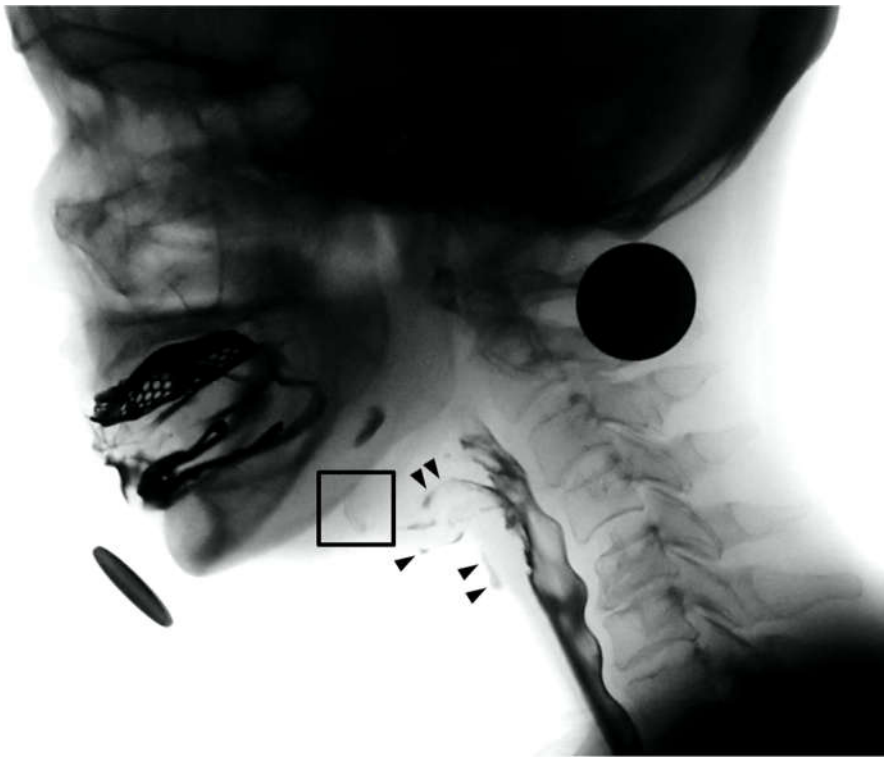

Fig. 1.3. The hyoid bone (black square) observed in the image of videofluoroscopic swallowing study. Liquid bolus was aspirated in the airway (arrow head).

1.2.2. Functional Data Analysis on Swallowing Motion

Functional data analysis is a statistical method for evaluation of time-series data that are recorded at discrete time intervals.[33] The basic idea of the functional data analysis is to express discrete observations arising time series as the functional form of data that represents the entire measured function as a single observation using basis expansion and smoothing methods.[34] The method can be used to analyze time series data of human motions for accurate estimation of parameters with effective noise reduction. It also allows quantitative analysis of the motion curves for group comparison.

Functional regression analysis is one of the promising applications in the field of functional data analysis. It may reveal differential time interval during the swallowing process with respect to displacement and velocity of the hyoid bone.[35] Although reduction in the hyoid displacement and velocity was observed previously, the kinematic features of the hyoid motion have not been investigated as swallowing process reflecting the nature of time-series data.[28] The functional linear regression model (FLR), which enables to conduct group comparison for swallowing motion in consideration of time-series data, can be useful to demonstrate novel features of hyoid motion in patients with dysphagia.

1.3. Prediction Models for Dysphagia

1.3.1. Importance of Prediction Models for Dysphagia

It is important to detect high-risk patients who are predicted to exhibit prolonged dysphagia in order to provide sufficient nutritional support and to prevent aspiration pneumonia. Particularly in stroke patients, long-term prognosis for dysphagia is necessarily predicted with high accuracy for gastrostomy tube placement, pneumonia prevention, applying intensive swallowing therapy, and guidance for patients and their families.[9,36,37] However, decision making for feeding tube placement can be highly variable due to lack of a systematic prediction method.[38,39] Delayed decision on the proper feeding route, or unnecessary restraint of oral intake can interfere with the outcome of swallowing function after stroke, since clinical decisions for tube placement are prone to be made during the time window of enhanced neuroplasticity.[40] Post-stroke dysphagia can also lead to increased institutionalization rate after discharge, and poor functional capacity in the long term.[11]

1.3.2. Previous Prediction Models for Dysphagia

Machine learning algorithms have been utilized in the field of swallowing researches for the hyoid bone tracking[41], normal swallow detection[42–44], and classifying pathologic swallow[45–48]. Particularly in diagnosing dysphagia, classifiers based on machine learning algorithms such as support vector machine and artificial neural networks were developed from diverse types of data including kinematic data from videofluoroscopy swallowing study (VFSS)[48], pressure data of high resolution impedance-manometry[47], vibration signals via an accelerometer[46], and swallowing

test scales by human evaluators[45]. The proposed classification algorithms showed high accuracy ranging from 79.8 to 92.7% for dysphagia detection. Despite the promising results of the previous studies, however, application of these prediction models in clinical practice needs consideration of medical approach in patient care. Dysphagia detection is crucial in nutrition and prevention of pneumonia. However, physicians usually require additional supportive information in evaluating swallowing function and establishing further plan: tongue control/bolus formation in oral phase of swallowing, aspiration mechanisms, sensation of pharyngeal areas, and coordination between swallowing-related structures. Information in these aspects can be obtained by conducting VFSS, which is the rationale that it is a standard evaluation tool for swallowing in clinical practice. Understanding the comprehensive information for overall swallowing process is essential for physicians to make a clinical decision for management and treatment plans.

To support decision-making for physicians in clinical practice, prediction of swallowing outcomes can be a more appropriate option than detection of dysphagia. Prediction of long-term swallowing recovery is important in management of post-stroke care. It enables clinicians to select appropriate evaluation plans, establish therapeutic strategies, and support counseling for patients and their families by individualizing a specific recovery trajectory.[49,50] Knowledge of factors for functional swallowing recovery is essential in developing a prognostic model for post-stroke dysphagia with high accuracy. For post-stroke dysphagia, numerous clinical and radiologic factors have been revealed to be associated with short-term (<1 month) swallowing recovery: older age[39,51], the African race[51], National Institutes of Health Stroke Scale (NIHSS)[39,51–54], initial risk of aspiration[39,54], initial impairment of oral intake[39], intubation[54], dysarthria[54], severe white matter

hyperintensities (WMH)[55], bilateral involvement[52,54], cortical lesions[51], and lesions of frontal area[53], insula[39,53,56–58], corona radiata[57], and internal capsule[56]. However, relatively few studies have investigated the prognostic factors for long-term (3-6 months) swallowing recovery: older age, sex, dysarthria, dysphonia, decreased gag reflex, initial dysphagia severity such as aspiration signs or symptoms, and bilateral involvement.[9,59,60] Particularly, there has been a lack of studies on anatomical locations or types of brain lesions for long-term swallowing recovery compared to those for short-term swallowing recovery in post-stroke dysphagia.

1.4. Research Objectives

The aim of the present study was to explore novel kinematic features of swallowing in patients with PD and stroke and to develop and validate machine learning-based prognostic models to predict functional swallowing status in patients with post-stroke dysphagia. First, kinematic analysis was conducted on patients with PD and ischemic stroke, respectively, to explore differential kinematic features of the hyoid motions during swallowing. Second, clinical and radiologic factors were explored to be associated with poor recovery of swallowing function at 6 months from stroke onset in patients with post-stroke dysphagia using survival analysis. Lastly, machine learning-based prognostic models were developed and validated to predict 6-month swallowing functional status using the relevant kinematic, clinical, and radiologic factors based on the kinematic and survival analyses.

2. Methods

2.1. Study Population and Data Collection

2.1.1. Parkinson's Disease

Total 69 subjects (23 patients with PD, 23 age- and sex-matched healthy elderly controls, and 23 healthy young controls) were analyzed in this study. The PD patients were diagnosed by neurologists between January 1, 2015 and December 31, 2016, and had mild to moderate dysphagia corresponding to scores of 5-6 on the American Speech–Language–Hearing Association's National Outcome Measurement System (ASHA NOMS), as assessed with VFSS. Patients who had undergone tracheostomy; those suffering from diseases such as stroke, brain tumor, head and neck cancer, and those without any swallowing reflex during the examination were excluded. Demographic data including sex, age, duration of disease, and duration of dysphagia were collected. Based on the VFSS findings, the videofluoroscopic dysphagia scale (VDS)[61] and ASHA NOMS swallowing scale were independently rated by two physiatrists. The data of healthy elderly and young controls were acquired from an anonymized VFSS data repository used in previous clinical studies.[62,63]

2.1.2. Ischemic Stroke

The study population included all consecutive patients with acute ischemic stroke between January 1, 2014 and June 31, 2018 and referred for VFSS due to swallowing

difficulty. All the medical records of the patients were retrospectively reviewed. Exclusion criteria were as follows: concomitant neurologic diseases which can result in swallowing dysfunction, age<19 years, tracheostomy, unconsciousness, premorbid dysphagia, and no records of brain magnetic resonance imaging (MRI). The data censored less than 4 months from patients with poor swallowing recovery were also excluded in consideration of developing classification model.

Demographic, neurologic, and swallowing characteristics were obtained from the patients including age (≥65 years), sex, stroke severity in terms of NIHSS at admission, stroke location, vascular territory of brainstem[64,65], stroke laterality, multifocal lesions, bilateral lesions at the corona radiata, basal ganglia, and/or internal capsule (CR/BG/IC) (Fig. 2.1), severity of WMH, clinical dysphagia scale (CDS)[66], and initial tube feeding. Stroke severity was categorized as mild (0–6), moderate (7–16), or severe (17–40) stroke according to the NIHSS.[67] Bilateral lesions of CR/BG/IC and severity of WMH were independently evaluated by two physiatrists. Bilateral lesions at CR/BG/IC include both acute and chronic lesions which were evaluated using diffusion weighted and fluid attenuated inversion recovery images. To differentiate cerebrospinal fluid-like foci from old lesions, cases that fulfilled three or more criteria were considered to be Virchow-Robin spaces and were therefore excluded. These criteria were as follows: 1) ≤2 mm; 2) smooth round, oval or linear shape; 3) without surrounding hyperintensity on FLAIR images; and 4) symmetric foci in bilateral hemispheres.[68,69] WMH in the periventricular and deep white matter were evaluated using fluid attenuated inversion recovery images of the initial MRI based on the Fazekas rating scale.[70] Severe WMH were defined as the sum of the Fazekas rating scale≥5 for paraventricular and deep white matter.[71] CDS was categorized into mild (<20) and moderate-to-severe (≥20) dysphagia. Tube

feeding status and CDS were evaluated by physiatrists at the initial VFSS. Initial VFSS refers to the first VFSS performed after stroke occurrence. The outcome of this study was the swallowing functional level at 6 months after stroke onset. When swallowing function did not necessitate tube placement or diet modification for nutrition, it was considered as good prognosis, whereas when either of them was needed, it was considered as poor prognosis.

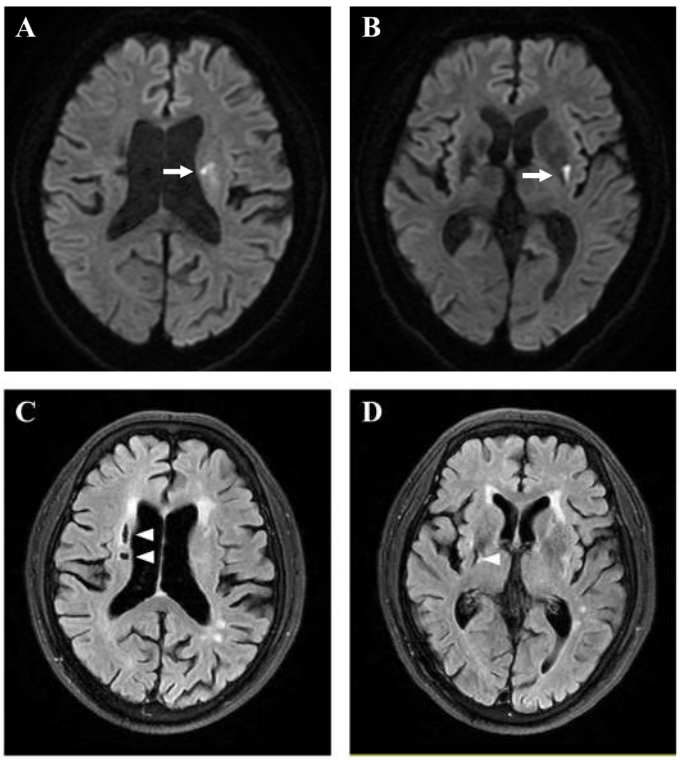

Fig. 2.1. Diffusion weighted and fluid attenuated inversion recovery images from a representative case who showed poor prognosis of post-stroke swallowing impairment. This 75-year-old male was diagnosed with acute infarction (arrow) at the corona radiata (A) and basal ganglia/internal capsule (B) of the left hemisphere, and old lesions (arrow head) at the corona radiata (C) and basal ganglia/internal capsule (D) of the right hemisphere. In the clinical evaluation for stroke and dysphagia severity, he showed 25 points on the clinical dysphagia scale with only 5 points of National Institutes of Health Stroke Scale. He was recommended to be fed via feeding tube for oral intake by videofluoroscopic swallowing study. After removing feeding tube at 4 months after stroke, he was still required to modify diet with food thickener.

2.2. Swallowing Assessments

All PD and stroke patients with swallowing difficulty were referred to physiatrists for swallowing evaluation after admission or through outpatient clinic. VFSS was conducted by physiatrists with the assistance of radiologic technologists using a C-arm or fluoroscope. The VFSS images were recorded at a rate of 30 images per second. The patients were seated in upright position and kept comfortable in a relaxed state. Before the VFSS, the patients were explained the overall process of examination and instructed to swallow the diluted barium solution in their usual manner after the verbal command. Variety of radiopaque food materials were administered in the patients including 2, 5, and/or 10 mL of 35% w/v diluted barium solutions, nectar thick liquid, honey thick liquid, soft blended diet (rice porridge), and/or steamed rice. Among these food materials, VFSS images for only 2 mL of a 35% w/v diluted barium solution were selected to be analyzed in the kinematic analyses to control volume and viscosity consistently.

VFSS enables physiatrists to determine appropriate food textures and types for dysphagia patients by visualizing dynamic motions of swallowing-related structures and airway protection in oral, pharyngeal, and esophageal phases of swallowing. Physiatrists established feeding strategies including tube placement and diet modification based on VFSS results to minimize the risk of aspiration and provide nutritional support. The feeding strategy was followed-up in patients with persistent dysphagia at the outpatient clinic or in the subsequent VFSSs. The interval of VFSS and outpatient clinic was every <4 weeks during the initial phase and gradually prolonged to 1-3 months considering the progress of swallowing recovery.

2.3. Swallowing Kinematic Analysis

2.3.1. Two-dimensional Motion Analysis

Displacement (HD) and velocity (HV) of the hyoid bone during swallowing were analyzed in this study. Positional data were collected from PD patients (n=23) and age- and sex-matched healthy elderly (n=23) and young (n=23) controls, and from stroke patients with poor prognosis (n=18) and age- and sex-matched stroke patients with good prognosis (n=18). To extract positional data of the hyoid bone from VFSS images, the swallowing motion analysis software, called spatio-temporal analyzer for motion and physiologic study (STAMPS; https://github.com/cmookj/stamps) was used in the present study.[72] According to this software, the local coordinate system was defined for each image and the origin was set at the anteroinferior vertex of the fourth cervical vertebral body (C4) (Fig. 2.2). The vertical axis was the line connecting the origin to the anteroinferior vertex of the second vertebral body (C2), while the horizontal axis was perpendicular to the vertical axis. For clinical understanding, the horizontal axis was set in the opposite direction to that of the conventional coordinate systems. The positional data of the hyoid bone, C2 and C4 vertebrae, and a reference object were obtained by manually marking the target structures in each frame. To adjust for variation in the size of the structures involved in swallowing, the measurements were scaled using the ratio between the true and observed-in-image lengths of the reference object. In the present study, a coin with a diameter of 23.5 mm was used as the reference object to calculate the scale factor and the length between C2 and C4 was adjusted to 40 mm for spatial normalization. The starting point of the hyoid bone was set as the origin of the coordinate axes for comparison of trajectories. The time laps between the start- and endpoints of the

swallowing process was interpolated to temporal values from 0 to 100 for temporal normalization.[73] The starting point was defined as the initiation of hyoid motion that resulted in a swallow or when the hyoid bone is located at the lowest during swallowing.[74] Terminal point was defined as the termination of hyoid motion after swallowing. Horizontal and vertical motions of the hyoid bone were defined as the motions along with horizontal and vertical axis. An angle that characterizes the direction of a straight line for the hyoid bone with respect to a positive horizontal axis was defined as the hyoid direction angle (Fig. 2.3). In this study, 5-20%ile duration was regarded as initial phase of swallowing to calculate the hyoid direction angle due to its high variability until 5%ile duration.

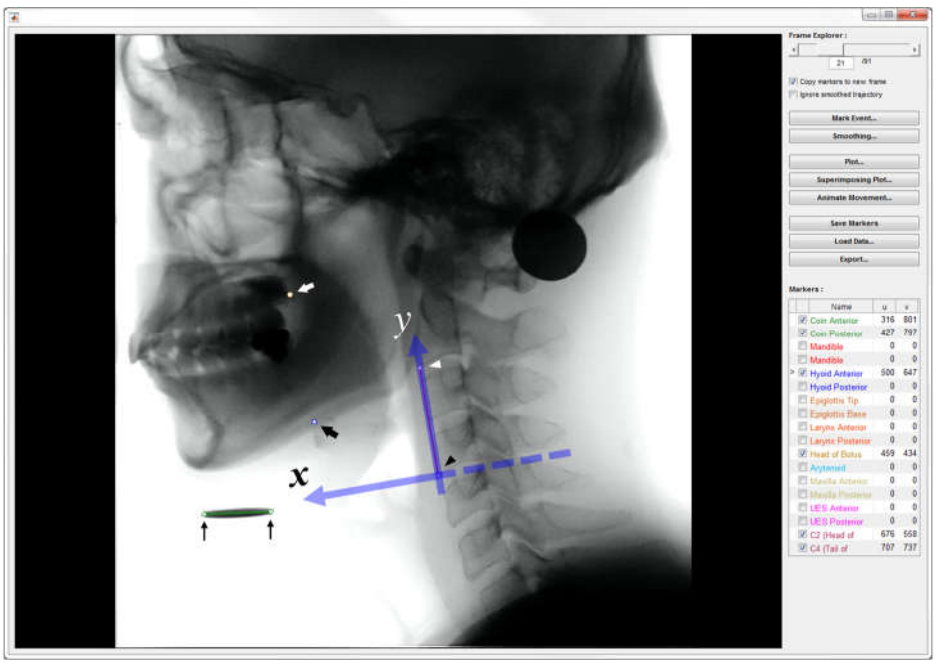

Fig. 2.2. The representation of a videofluoroscopic image and corresponding coordinate systems using the swallowing motion analysis software. The horizontal axis is opposite in direction to that of the conventional coordinate systems for clinical understanding. The positional data of the hyoid bone (black solid arrow), liquid bolus (white solid arrow), second (white arrowhead) and fourth cervical vertebral bodies (black arrowhead), and a reference metal object (thin black arrow) were obtained by manually marking the target structures in the software.

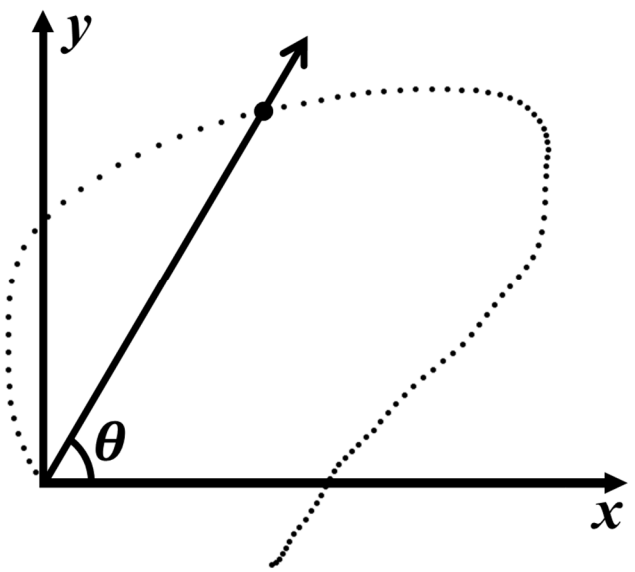

Fig. 2.3. A Hyoid direction angle during swallowing. The direction angle was defined as an angle that characterizes the direction of a straight line for the hyoid bone with respect to a positive horizontal axis.

2.3.2. Functional Regression Analysis

Positional data, obtained at discrete time points, can be mapped into sets of measurements along a continuum, called functional data, using a linear combination of basis functions, ϕ_k, which are B-spline functions in this study.[75,76] For the given true functions of $X_i(t)$ in the *i*-th subject, observation value with noise can be represented as $W_i(t) = X_i(t) + \epsilon_i(t)$ at time point *t*. $X_i(t)$ is estimated as $\widehat{X_i}(t) = \sum_{k=1}^{K} \widehat{c_{ik}}\, \phi_k(t)$. In general, this form can be expanded and represented as the concurrent regression model $y(t) = Z(t)\beta(t) + \epsilon(t)$, which consists of the functional matrix Z and regression coefficient function β for a given response function y.

In FLR, the response function y can be represented as

$$y_{ijk}(t) = \mu(t) + (-1)^i \alpha(t) + \beta_{ij}(t) + \epsilon_{ijk}(t), \qquad (1)$$

where the output measure consists of a grand mean effect $\mu(t)$, mean difference $\alpha(t)$ between groups (i = 1, 2), effect of each subject $\beta_{ij}(t)$, and residual function $\epsilon_{ijk}(t)$. Smoothing for noise reduction and imposition of constraints on β_{ij} for identifiability of the model are also performed in the data analysis. Roughness penalties are used for regularization to prevent overfitting. To calculate regression coefficients, the penalized sum of squares (PENSSE) is minimized with the least-squares approach. The PENSSE_λ is minimized with penalty coefficient λ and operator L. This step consists of the two terms shown below.

$$\text{PENSSE}_\lambda(\alpha, \beta) = \sum [y_i - \alpha - \int x_i(t)\beta(t)dt]^2 + \lambda \int [L\,\beta(t)]^2 dt. \qquad (2)$$

In the present study, generalized cross-validation was adopted to identify the appropriate number of basis functions and the lambda value for penalization. Intergroup differences in hyoid displacement were fitted through FLR. Hyoid velocity was approximated using the symmetric difference quotient as the sequence of the finite differences of the displacement. For all measures along time t, the difference in the hyoid motion was considered to be significant when the 95% confidence intervals of regression coefficients did not present with the value zero. Statistical significance was set at $P<0.05$. The analyzing process was performed using R version 3.4.2 (The R Foundation, Vienna, Austria) with the *fda* package. The two-dimensional hyoid trajectories were illustrated using Matlab R2019a (The Mathworks, Natick, MA, USA)

2.4. Statistical Analysis

In PD patients, analyses for the demographic factors, VDS score, and maximal values of HD/HV were performed using the independent-samples t-test. The chi-squared test or Fisher's exact test was used to analyze proportions of subjects with abnormal VDS parameters: triggering of pharyngeal swallow, vallecular residue, laryngeal elevation, pyriform sinus residue, coating on the pharyngeal wall, pharyngeal transit time, and aspiration. Pearson or Spearman correlation coefficient was obtained to analyze the correlation between the VDS score and maximal values of HD/HV. The maximal values of HD/HV according to the VDS parameters and ASHA NOMS swallowing scale were analyzed using independent samples t-test or Mann-Whitney U test.

Between stroke patients with good and poor prognosis of swallowing function, the demographic, neurologic, and swallowing characteristics were compared using independent-samples t-test for continuous variables, and chi-squared test or Fisher's exact test for categorical variables. The maximal values of HD/HV and mean values of direction angle for 5-20%ile duration were compared between the age- and sex-matched stroke patients using independent sample t-test or Mann-Whitney U test. In the survival analysis, the event of interest was defined as the first successful return to pre-stroke diet. The time to the first return to pre-stroke diet was analyzed using the Kaplan-Meier method, and covariates including the demographic, neurologic, and swallowing characteristics were analyzed using a stratified log-rank test. To identify potential prognostic factors, Cox proportional-hazards models were used for each covariate. Factors with P-value<0.2 were used as covariates in the multivariate analysis of Cox proportional-hazards models, and the

forward variable selection method was applied to control for multicollinearity. The statistical analyses were conducted using SPSS software (version 19; SPSS Inc, Chicago, IL, USA), and the significance level was set at $P<0.05$.

2.5. Development and Validation of the Machine Learning-based Prognostic Model

2.5.1. XGBoost

For the development of the prognostic model for 6-month swallowing recovery, an eXtreme Gradient Boosting (XGBoost) model was used to classify stroke patients into those with good and poor swallowing prognosis. XGBoost is one of the gradient boosting machines which have shown to give state-of-the-art results on many standard classifications in a wide range of practical applications.[77] Gradient tree boosting algorithm refers to a family of ensemble methods in which each weak classifier is combined as weighted averages into single strong classifier using a gradient-descent based formulation.[78] The learning procedure sequentially fits new models to produce more accurate estimates of the response variable.[78] The main difference between a boosting algorithm and conventional machine learning techniques is that optimization is held out in the function space.[78]

XGBoost classifier is an ensemble method using a gradient tree boosting algorithm with regularization term to control the complexity of the tree to get simpler model and avoid over-fitting.[79] In this algorithm, a gradient descent method is utilized to minimize the loss when new models are added in an iterative fashion.

$$\hat{y}_i = \sum_{k=1}^{K} f_k(x_i), f_k \in F, \tag{3}$$

where x_i represents the i-th sample in the training dataset and $F = \{f(x) = w_{q(x)}\}(q : \mathbb{R}^m \rightarrow T, w \in \mathbb{R}^T)$ is the space of regression trees.[77] Each tree $f(x_i)$

corresponds to a structure parameter q that maps a sample to the corresponding leaf index. T is the number of leaves in the tree, w is the leaf weights, and K is the number of trees that are utilized to estimate the output. The results of the prediction is the sum of the scores predicted by K trees. The loss function is minimized by greedily finding the penalty, which is given by the following formula as

$$L\left(\theta\right) = \sum_{i=1}^{N} l(y_i, \hat{y}_i) + \sum_{k=1}^{K} \Omega\ (f_k). \quad (4)$$

Here, $l()$ represents the loss function which can be differentiated to measure whether the model is suitable for training dataset, and $\Omega(f_k)$ is the penalty to punish the complexity of the model.

In this study, the prognostic model for 6-month swallowing recovery based on the XGBoost model was constructed using the clinical, radiologic, and kinematic variables relevant to functional recovery of post-stroke dysphagia. The clinical and radiologic variables with P-value<0.2 in the Cox proportional-hazards analyses of the survival model and all of the kinematic variables for the hyoid motion during swallowing were included as the feature variables in the XGBoost model. The objective of the XGBoost model was to perform binary classification among two classes: good prognosis which refers to swallowing functional status not necessitating tube placement or diet modification for nutrition at 6 months after stroke onset, and poor prognosis which refers to swallowing functional status necessitating tube placement or diet modification. Additionally, other machine learning algorithms including support vector machine, random forest, and artificial neural networks were used to benchmark the performance of the developed XGBoost model after hyperparameter optimization.

2.5.2. Validation and Evaluation of the Proposed Prognostic Models

Training and validation processes were shown in Fig. 2.4. The whole dataset was divided into training and test dataset by the ratio of 75:25%, respectively. For the kinematic variables of the hyoid motion, feature scaling was performed based on the training dataset using min-max normalization. Due to high-dimensional and relatively small samples, recursive feature elimination was utilized as an effective feature selection method for the feature variables including clinical, radiologic, and kinematic variables. After those processes, the training set was randomly partitioned into 5 subsets with almost equal size for 5-fold cross validation. One partition was selected as the validation set and the rest of the partitions were used to train the predictive models. To reduce the error cost by mitigating the class imbalance between the patients with good and poor prognosis in the data set, adaptive synthetic sampling, called ADASYN, was implemented for the minority class as an oversampling algorithm.[80] ADASYN is a systematic method of oversampling to adaptively create different amounts of synthetic data which need to be generated for minority class to compensate for the skewed distributions according to their density distributions.[80,81] In learning and validation process, 5-fold cross validation was used during the process of oversampling by generating synthetic samples for only training partitions to avoid overfitting and over-optimistic estimates.[82] It can prevent contamination of the synthetic samples generated from the training partitions into the test set. Finally, the model performance was evaluated for test set using three metrics: an area under the receiver operating characteristic (ROC) curve, F1 score, and Matthews correlation coefficient (MCC), which were regarded as good options

for metrics to assess the predictive performance of the models which constructed from the imbalanced data set.[83–85] F1 score is the harmonic mean of the precision and recall ranging from 0 to 1. MCC has been widely used for evaluation of binary classification in imbalanced data.[83] MCC is in essence a correlation coefficient value ranging from -1 to 1, and is defined in terms of true positive (TP), true negative (TN), false positive (FP), and false negative (FN) as follows.

$$MCC = \frac{TP \times TN - FP \times FN}{\sqrt{(TP + FP)(FP + FN)(TN + FP)(TN + FN)}} \quad (5)$$

The whole process of analyses was performed using R version 3.4.2 (The R Foundation, Vienna, Austria) with the *xgboost*, *caret*, *keras*, and *kernlab* packages for development and validation of XGBoost and other machine learning models, and the *imbalance* package for oversampling of minority class.

2.6. Study Approval

This study was approved by the institutional review board (IRB No. 1802-128-927, IRB No. 1707-178-875) and informed consent was exempted from retrospective review. It was performed in accordance with all relevant guidelines and regulations.

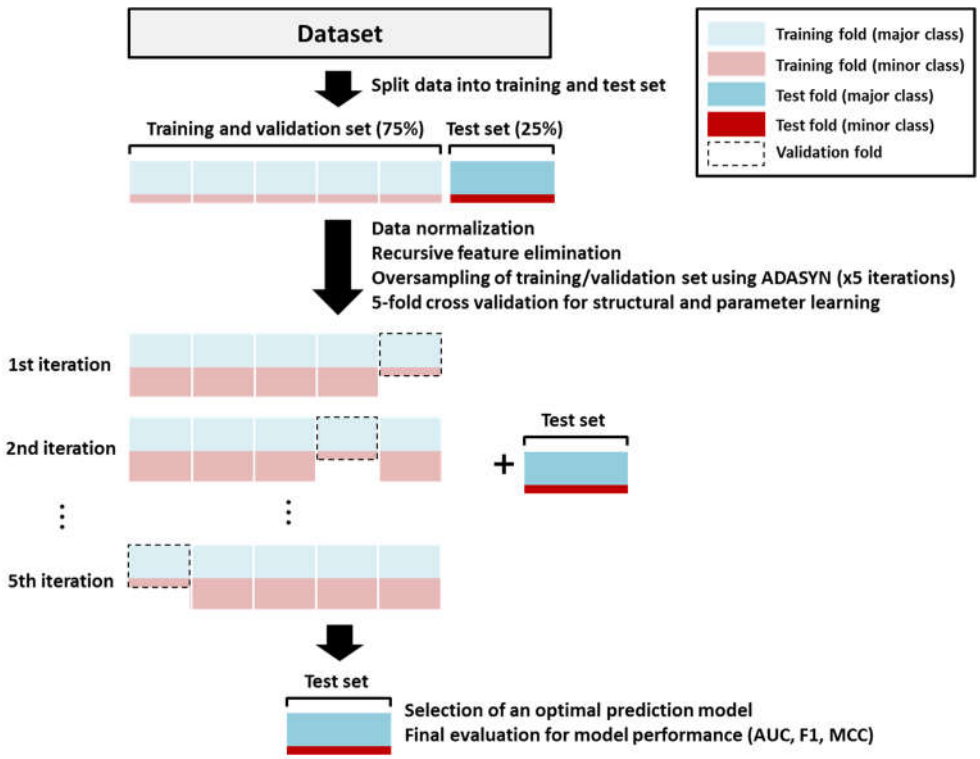

Fig. 2.4. The illustration of overall process for 5-fold cross-validation with oversampling and model evaluation

3. Results

3.1. Swallowing Kinematic Characteristics in Patients with Parkinson's disease

3.1.1. Clinical Characteristics

Table 1 and 2 summarize the clinical characteristics and VDS parameters in the PD patients, healthy elderly controls, and healthy young controls included in the present study. The VDS score was significantly different between PD patients and healthy elderly controls (24.24±12.41 *vs.* 6.54±7.28, $P<0.001$). The proportions of the subjects with abnormal VDS parameters were significantly different with respect to vallecular residue ($P=0.011$), coating on the pharyngeal wall ($P<0.001$), and aspiration ($P<0.001$) between the two groups. No significant difference was observed between healthy elderly and young controls for both VDS score and proportions of each parameter.

Table 3.1. Clinical characteristics of patients with Parkinson's disease (PD), and healthy elderly and young controls

	PD (n=23)	Elderly (n=23)	*P* (PD *vs.* Elderly)	Young (n=23)	*P* (Elderly *vs.* Young)
Age (year)	70.8±6.6	68.6±5.0	0.213	36.0±12.8	<0.001
Sex (male)	12 (52.2)	12 (52.2)	1.000	11 (47.8)	1.000
ASHA-NOMS scale (5/6/7)	10/13/0	0/0/23	<0.001	0/0/23	1.000
Disease duration (months)	111.7 ± 61.3	-	-	-	-
Dysphagia duration (months)	16.96 ± 28.4	-	-	-	-

Values are presented as mean ± standard deviation, or number (percent).

Table 3.2. Parameters of pharyngeal swallowing based on the videofluoroscopic dysphagia scale (VDS) in patients with Parkinson's disease (PD), and healthy elderly and young controls

	PD (n=23)	Elderly (n=23)	*P* (PD *vs.* Elderly)	Young (n=23)	*P* (Elderly *vs.* Young)
VDS score	24.24±12.41	6.54±7.28	<0.001*	3.50±5.25	0.111
Triggering of pharyngeal swallow			0.109		-
Normal	19 (82.6)	23 (100.0)		23 (100.0)	
Delayed	4 (17.4)	0 (0.0)		0 (0.0)	
Vallecular residue			0.011*		0.134
None	2 (8.7)	7 (30.4)		12 (52.2)	
<10%	13 (56.5)	16 (69.6)		11 (47.8)	
10-50%	5 (21.7)	0 (0.0)		0 (0.0)	
>50%	3 (13.0)	0 (0.0)		0 (0.0)	
Laryngeal elevation			0.187		1.000
Normal	18 (78.3)	22 (95.7)		23 (100.0)	
Impaired	5 (21.7)	1 (4.3)		0 (0.0)	

Pyriform sinus residue			0.293		0.536
None	10 (43.5)	14 (60.9)		16 (69.6)	
<10%	10 (43.5)	9 (39.1)		7 (30.4)	
10-50%	2 (8.7)	0 (0.0)		0 (0.0)	
>50%	1 (4.3)	0 (0.0)		0 (0.0)	
Coating on the pharyngeal wall			0.001*		0.699
No	7 (30.4)	18 (78.3)		20 (87.0)	
Yes	16 (69.6)	5 (21.7)		3 (13.0)	
Pharyngeal transit time			0.109		-
≤1.0 s	19 (82.6)	23 (100.0)		23 (100.0)	
>1.0 s	4 (17.4)	0 (0.0)		0 (0.0)	
Aspiration			<0.001*		0.233
None	3 (13.0)	20 (87.0)		23 (100.0)	
Supraglottic penetration	9 (39.1)	3 (13.0)		0 (0.0)	
Subglottic aspiration	11 (47.8)	0 (0.0)		0 (0.0)	

Values are presented as mean ± standard deviation, or number (percent).

3.1.2. Functional Regression Analysis for Hyoid Displacement

Fig. 3.1 shows the mean two-dimensional trajectories of the hyoid bone during swallowing in PD patients, healthy elderly and young controls. The mean HDs in the horizontal and vertical planes for patients with PD, healthy elderly, and healthy young controls are shown in Fig. 3.2 (A, D). The regression coefficient functions representing intergroup differences for the horizontal and vertical HDs over time between the PD patients and healthy elderly controls are shown in Fig. 3.2 (B, E), and those between the healthy elderly and young controls in Fig. 3.2 (C, F), respectively. Horizontal HD differed significantly between patients with PD and healthy elderly controls over the initial backward (9^{th}–15^{th} percentiles) and forward motions (33^{rd}–69^{th} percentiles). Vertical HD did not show any significant difference over time between the two groups. Between the healthy elderly and young controls, significant differences were observed in the horizontal and vertical HDs at the 51^{st}-57^{th} and 44^{th}-62^{nd} percentiles, respectively.

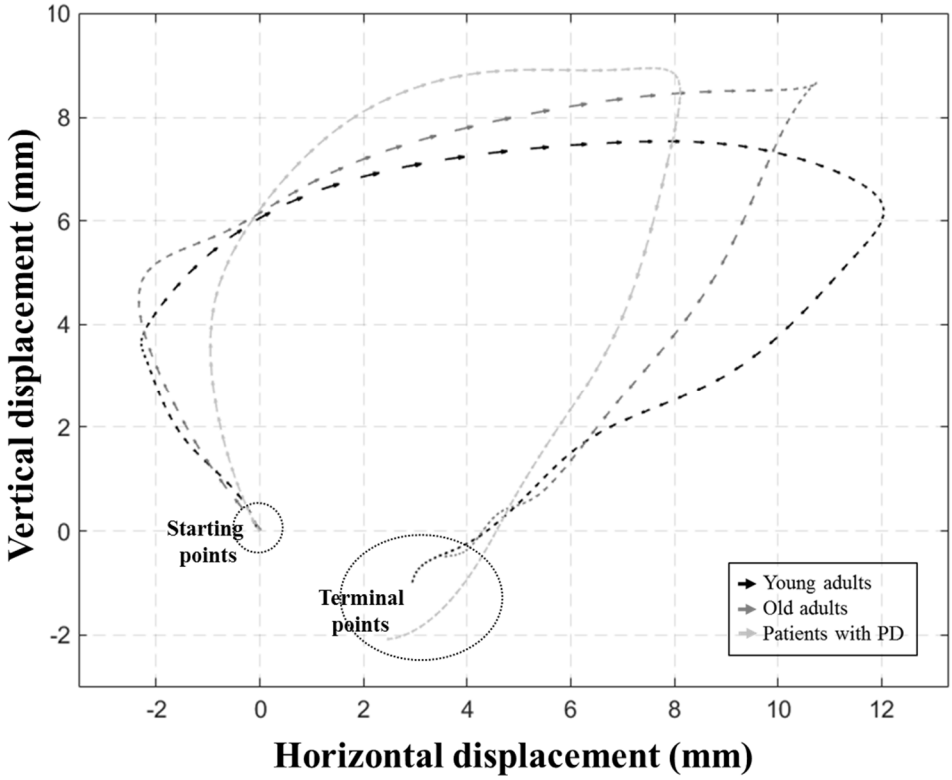

Fig. 3.1. The mean two-dimensional trajectories of the hyoid bone during swallowing in patients with Parkinson′s disease (PD), healthy elderly and young controls.

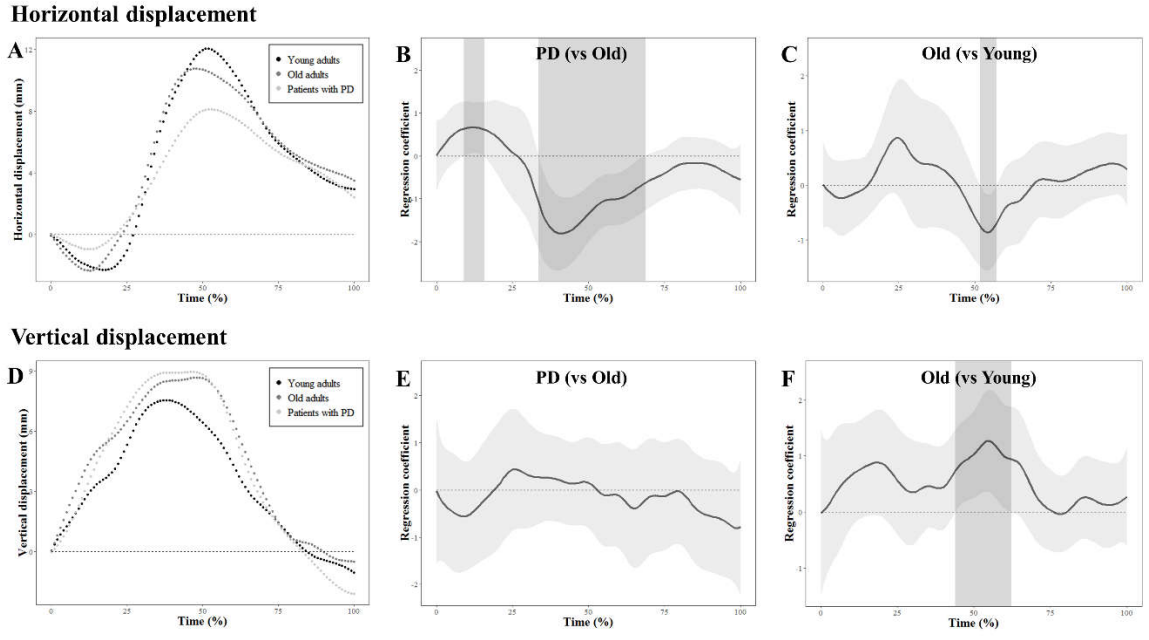

Fig. 3.2. Results of functional regression analysis for horizontal and vertical hyoid displacements. Mean trajectories are illustrated for the horizontal (A) and vertical (D) displacements in patients with Parkinson's disease (PD), healthy elderly and young controls. Estimated regression coefficient functions with 95% confidence intervals are shown for the horizontal and vertical displacements between patients with PD and healthy elderly controls (B, E), and between healthy elderly and young controls (C, F). The light gray zones denote the time interval where the mean difference is significant between the groups.

3.1.3. Functional Regression Analysis for Hyoid Velocity

The mean HVs in the horizontal and vertical planes for patients with PD, healthy elderly, and healthy young controls are shown in Fig. 3.3 (A, D). The regression coefficient functions representing intergroup differences for the horizontal and vertical HVs over time between patients with PD and healthy elderly controls are shown in Fig. 3.3 (B, E), and those between the healthy elderly and healthy young controls in Fig. 3.3 (C, F), respectively. The HV showed significant differences between patients with PD and healthy elderly controls at the 0-6^{th}/27^{th}-37^{th}/47^{th}-53^{rd}/63^{rd}-67^{th}/93^{rd}-97^{th} percentiles in the horizontal plane, and the 0-3^{rd}/83^{rd}-87^{th} percentiles in the vertical plane. Between the healthy elderly and young controls, the horizontal and vertical HVs were significantly different at the 19^{th}-23^{rd}/46^{th}-51^{st} percentiles, and 3^{rd}-6^{th} percentiles, respectively.

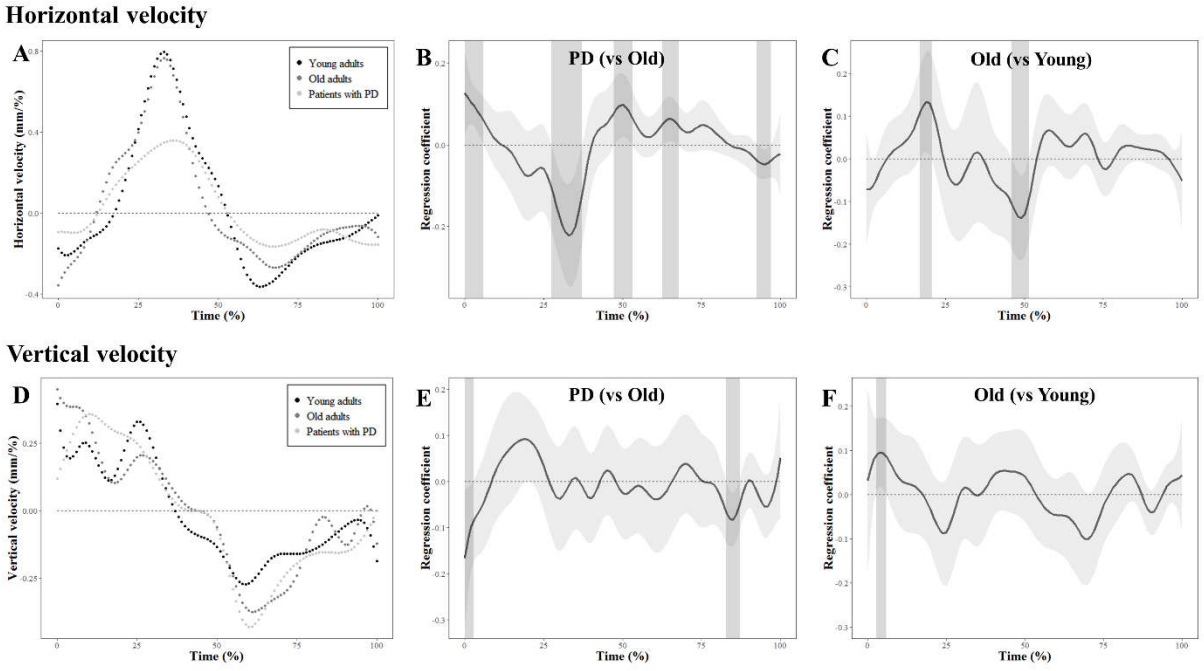

Fig. 3.3. Results of functional regression analysis for horizontal and vertical hyoid velocities. Mean trajectories are illustrated for the horizontal (A) and vertical (D) velocities in patients with Parkinson's disease (PD), healthy elderly and young controls. Estimated regression coefficient functions with 95% confidence intervals are shown for the horizontal and vertical velocities between patients with PD and healthy elderly controls (B, E), and between healthy elderly and young controls (C, F). The light gray zones denote the time interval where the mean difference is significant between the groups.

3.1.4. Analysis for Maximal Values of Hyoid Kinematic Parameters

Table 3.3 and 3.4 shows the results of analyses for the maximal values of HD and HV. Both HD and HV of the horizontal plane differed significantly in the initial backward (P=0.006, P<0.001, respectively), and forward (P=0.008, P<0.001, respectively) motions between patients with PD and healthy elderly controls. In the vertical plane, only HV showed significant difference between the two groups (P=0.001). The HD and HV of the horizontal and vertical planes were not significantly different between the healthy elderly and young controls.

For the maximal values of HD and HV, the VDS score demonstrated a significant positive correlation with the horizontal HD/HV in the initial backward motion (r=0.353, P=0.003; r=0.481, P<0.001), and a significant negative correlation with the horizontal HD/HV in the forward motion (r=-0.460, P<0.001; r=-0.537, P<0.001). In the subgroup analysis for PD patients, the VDS score was significantly correlated with the horizontal HD (ρ=-0.498, P=0.016) and HV (ρ=-0.428, P=0.042) in the forward motion. Table 3.5-3.7 showed the significant associations between HD/HV and multiple VDS parameters patients with PD, and healthy elderly and young controls. Additionally, the significant associations between HD/HV and multiple VDS parameters in the PD patients are shown in Supplemental Table 1-3. Among the PD patients, only vertical HV was significantly different between the groups with ASHA NOMS swallowing scale 5 and 6 (n=10, 0.61±0.17 *vs.* n=13, 0.79±0.18 mm/%ile, P=0.022).

Table 3.3. Results of analysis for the maximal displacement of the hyoid bone in patients with Parkinson's disease, and healthy elderly and young controls

	PD (n=23)	Elderly (n=23)	*P* (PD *vs.* Elderly)	Young (n=23)	*P* (Elderly *vs.* Young)
Maximal horizontal displacement (mm)					
Backward	-1.83± 1.21	-3.49±2.14	0.006*	-3.46±1.78	0.999
Forward	8.93±3.00	12.30±4.33	0.008*	13.5±3.50	0.488
Maximal vertical displacement (mm)					
Upward	11.60±5.12	10.50±5.32	0.756	9.46±5.31	0.763
Time to maximal displacement (%ile)					
Horizontal, backward	16.22±9.30	14.97±7.42	0.844	18.56±5.87	0.258
Horizontal, forward	52.61±11.55	51.07±12.13	0.876	50.90±7.84	0.998
Vertical, upward	38.40±15.60	38.44±11.95	0.999	41.23±9.74	0.736

Values are presented as mean ± standard deviation.

**P*-value<0.05.

Table 3.4. Results of analysis for the maximal velocity of the hyoid bone in patients with Parkinson's disease, and healthy elderly and young controls

	PD (n=23)	Elderly (n=23)	*P* (PD *vs.* Elderly)	Young (n=23)	*P* (Elderly *vs.* Young)
Maximal horizontal velocity (mm/%ile)					
Backward	-0.20±0.03	-0.61±0.32	<0.001*	-0.59±0.31	0.972
Forward	0.63±0.27	1.26±0.47	<0.001*	1.38±0.47	0.569
Maximal vertical velocity (mm/%ile)					
Upward	0.71±0.20	1.23±0.55	0.001*	1.00±0.60	0.243
Time to maximal velocity (%ile)					
Horizontal, backward	7.29±8.24	3.59±6.14	0.139	5.98±6.08	0.418
Horizontal, forward	32.26±8.68	29.35±7.30	0.426	33.67±6.98	0.151
Vertical, upward	20.65±13.08	12.11±11.89	0.060	13.38±12.52	0.936

Values are presented as mean ± standard deviation.

**P*-value<0.05.

Table 3.5. Horizontal hyoid displacement (HD) and velocity (HV) in the initial backward motion associated with parameters of the videofluoroscopic dysphagia scale in patients with Parkinson's disease and healthy controls (N=69)

	n	HD (mm)	*P*	HV (mm/%ile)	*P*
Triggering of pharyngeal swallow			0.028*		0.013*
Normal	65	-3.04±1.88		-0.48±0.32	
Delayed	4	-1.10±1.24		-0.14±0.15	
Vallecular residue			0.026*		0.005*
None	21	-3.45±1.15		-0.56±0.30	
<10%	40	-2.90±2.20		-0.48±0.33	
10-50%	5	-2.04±1.26		-0.19±0.08	
>50%	3	-1.02±1.18		-0.12±0.11	
Laryngeal elevation			0.469		0.010*
Normal	63	-2.98±1.90		-0.49±0.32	
Impaired	6	-2.31±1.87		-0.20±0.21	
Pyriform sinus residue			0.283		0.552
None	40	-3.18±1.80		-0.52±0.36	
<10%	26	-2.65±2.10		-0.41±0.25	

10-50%	2	-1.76±0.62		-0.26±0.04	
>50%	1	-2.34		-0.24	
Coating on the pharyngeal wall			0.046*		0.005*
No	45	-3.26±1.95		-0.54±0.34	
Yes	24	-2.30±1.66		-0.32±0.22	
Pharyngeal transit time			0.028*		0.013*
≤1.0 s	65	-3.04±1.88		-0.48±0.32	
>1.0 s	4	-1.10±1.24		-0.14±0.15	
Aspiration			0.010*		<0.001*
None	46	-3.40±2.00		-0.57±0.32	
Supraglottic penetration	12	-2.10±1.30		-0.31±0.20	
Subglottic aspiration	11	-1.83±1.19		-0.18±0.09	

Values are presented as mean ± standard deviation.

*P-value<0.05.

Table 3.6. Horizontal hyoid displacement (HD) and velocity (HV) in the forward motion associated with parameters of the videofluoroscopic dysphagia scale in patients with Parkinson's disease and healthy controls (N=69)

	n	HD (mm)	*P*	HV (mm/%ile)	*P*
Triggering of pharyngeal swallow			0.029*		0.005*
Normal	65	11.82±4.08		1.13±0.51	
Delayed	4	7.71±2.80		0.45±0.14	
Vallecular residue			0.001*		<0.001*
None	21	12.32±4.18		1.36±0.55	
<10%	40	12.25±3.72		1.07±0.45	
10-50%	5	6.74±1.19		0.51±0.12	
>50%	3	5.52±0.35		0.33±0.04	
Laryngeal elevation			0.070		0.058
Normal	63	11.87±4.02		1.12±0.52	
Impaired	6	8.53±4.25		0.70±0.41	
Pyriform sinus residue			0.161		0.108
None	40	12.46±4.26		1.18±0.52	
<10%	26	10.53±3.70		1.02±0.52	

10-50%	2	10.44±2.80		0.62±0.10	
>50%	1	5.88		0.36	
Coating on the pharyngeal wall			0.003*		0.003*
No	45	12.62±4.26		1.22±0.51	
Yes	24	9.62±3.04		0.84±0.46	
Pharyngeal transit time			0.029*		0.005*
≤1.0 s	65	11.82±4.08		1.13±0.51	
>1.0 s	4	7.71±2.80		0.45±0.14	
Aspiration			0.004*		<0.001*
None	46	12.69±3.99		1.28±0.50	
Supraglottic penetration	12	10.36±3.68		0.83±0.38	
Subglottic aspiration	11	8.26±3.01		0.57±0.27	

Values are presented as mean ± standard deviation.

*P-value<0.05.

Table 3.7. Vertical hyoid displacement (HD) and velocity (HV) associated with parameters of the videofluoroscopic dysphagia scale in patients with Parkinson's disease and healthy controls (N=69)

	n	HD (mm)	*P*	HV (mm/%ile)	*P*
Triggering of pharyngeal swallow			0.174		0.013*
Normal	65	10.73±5.34		1.01±0.52	
Delayed	4	7.66±2.05		0.49±0.19	
Vallecular residue			0.792		0.212
None	21	9.96±5.98		0.94±0.45	
<10%	40	10.74±5.16		1.06±0.58	
10-50%	5	10.19±2.62		0.70±0.17	
>50%	3	12.72±6.00		0.69±0.31	
Laryngeal elevation			0.749		0.125
Normal	63	10.50±5.36		0.10±0.53	
Impaired	6	11.00±4.28		0.07±0.26	
Pyriform sinus residue			0.240		0.983
None	40	9.74±5.39		0.99±0.54	
<10%	26	11.40±5.01		0.98±0.53	

10-50%	2	11.68±1.96		0.87±0.18	
>50%	1	18.64		1.00	
Coating on the pharyngeal wall			0.287		0.924
No	45	10.05±5.48		0.99±0.52	
Yes	24	11.48±4.76		0.97±0.54	
Pharyngeal transit time			0.174		0.013*
≤1.0 s	65	10.73±5.34		1.01±0.52	
>1.0 s	4	7.66±2.05		0.49±0.19	
Aspiration			0.345		0.066
None	46	10.18±5.38		1.08±0.58	
Supraglottic penetration	12	9.66±3.35		0.82±0.36	
Subglottic aspiration	11	13.05±6.04		0.75±0.24	

Values are presented as mean ± standard deviation.

*P-value<0.05.

3.2. Swallowing Kinematic Characteristics in Patients with Ischemic Stroke

3.2.1. Clinical Characteristics

Among the 137 patients with acute ischemic stroke (Table 3.8) who were candidates for the swallowing kinematic study according to the inclusion criteria, 18 patients with poor prognosis (no recovery to pre-stroke status at 6 months) and 18 age- and sex-matched patients with good prognosis (recovery to pre-stroke status at 6 months) were selected. Table 3.9 summarizes the clinical characteristics in the age- and sex-matched stroke patients with good and poor prognosis for swallowing function. Mean age of the two groups was not different significantly (good prognosis, 73.9±8.9; poor prognosis, 73.6±8.9, P=0.912). Among the clinical and radiologic variables, initial tube feeding was the only factor to be different significantly between two groups (good prognosis, 1 (5.6%); poor prognosis, 14 (77.8%); P<0.001).

Table 3.8. Clinical characteristics in patients with post-stroke dysphagia (N=137)

	Total (N=137)	Good prognosis (n=113)	Poor prognosis (n=24)	*P*-value
Age≥65	100 (73.0)	78 (69.0)	22 (91.7)	0.023*
Sex				0.008*
Male	69 (50.4)	51 (45.1)	18 (75.0)	
Female	68 (49.6)	62 (54.9)	6 (25.0)	
NIHSS at admission				0.116
Mild (0-6)	48 (36.1)	35 (32.1)	13 (54.2)	
Moderate (7-16)	59 (44.4)	52 (47.7)	7 (29.2)	
Severe (17-40)	26 (19.5)	22 (20.2)	4 (16.7)	
Vascular territory of brainstem				
Anteromedial territory	14 (10.2)	11 (9.7)	3 (12.5)	0.712
Anterolateral territory	12 (8.8)	7 (6.2)	5 (20.8)	0.021*
Lateral territory	13 (9.5)	10 (8.8)	3 (12.5)	0.700
Posterior territory	1 (0.7)	1 (0.9)	0 (0.0)	1.000
Lesion laterality				0.152
Right	56 (40.9)	50 (44.2)	6 (25.0)	
Left	67 (48.9)	51 (45.1)	16 (66.7)	
Bilateral	14 (10.2)	12 (10.6)	2 (8.3)	
Lesion location				
Frontal lobe	64 (46.7)	56 (49.6)	8 (33.3)	0.148
Parietal lobe	49 (35.8)	42 (37.2)	7 (29.2)	0.458
Temporal lobe	38 (27.7)	31 (27.4)	7 (29.2)	0.863
Occipital lobe	14 (10.2)	13 (11.5)	1 (4.2)	0.281
CR	53 (38.7)	41 (36.3)	12 (50.0)	0.210

BG/IC	54 (39.4)	42 (37.2)	12 (50.0)	0.243
Insula	33 (24.1)	25 (22.1)	8 (33.3)	0.243
Thalamus	9 (6.6)	7 (6.2)	2 (8.3)	0.657
Midbrain	2 (1.5)	2 (1.8)	0 (0.0)	1.000
Pons	15 (10.9)	12 (10.6)	3 (12.5)	0.727
Medulla oblongata	15 (10.9)	11 (9.7)	4 (16.7)	0.300
Cerebellum	12 (8.8)	10 (8.8)	2 (8.3)	1.000
Multifocal lesions	18 (13.1)	16 (14.2)	2 (8.3)	0.739
Bilateral lesions at CR/BG/IC	30 (21.9)	17 (15.0)	13 (54.2)	<0.001*
Severe white matter hyperintensities	22 (16.1)	14 (12.4)	8 (33.3)	0.011*
Clinical dysphagia scale≥20	49 (35.8)	33 (29.2)	16 (66.7)	0.001*
Initial tube feeding	27 (19.7)	10 (8.8)	17 (70.8)	<0.001*

BG, basal ganglia; CR, corona radiata; IC, internal capsule; NIHSS, National Institutes of Health Stroke Scale.

**P*-value<0.05

Table 3.9. Clinical characteristics of age- and sex-matched stroke patients with good and poor prognosis for swallowing function (n=36)

	Good prognosis (n=18)	Poor prognosis (n=18)	*P*-value
Age≥65	16 (88.9)	16 (88.9)	1.000
Sex			1.000
Male	12 (66.7)	12 (66.7)	
Female	6 (33.3)	6 (33.3)	
NIHSS at admission			0.274
Mild (0-6)	6 (35.3)	11 (61.1)	
Moderate (7-16)	9 (52.9)	5 (27.8)	
Severe (17-40)	2 (11.8)	2 (11.1)	
Vascular territory of brainstem			
Anteromedial territory	0 (0.0)	3 (16.7)	0.229
Anterolateral territory	1 (5.6)	5 (27.8)	0.177
Lateral territory	1 (5.6)	3 (16.7)	0.603
Posterior territory	0 (0.0)	0 (0.0)	-
Lesion laterality			0.131
Right	7 (38.9)	3 (16.7)	
Left	7 (38.9)	13 (72.2)	
Bilateral	4 (22.2)	2 (11.1)	
Lesion location			
Frontal lobe	8 (44.4)	3 (16.7)	0.146
Parietal lobe	6 (33.3)	3 (16.7)	0.443
Temporal lobe	4 (22.2)	4 (22.2)	1.000
Occipital lobe	4 (22.2)	1 (5.6)	0.338
CR	7 (38.9)	9 (50.0)	0.502

BG/IC	6 (33.3)	9 (50.0)	0.310
Insula	2 (11.1)	5 (27.8)	0.402
Thalamus	2 (11.1)	2 (11.1)	1.000
Midbrain	0 (0.0)	0 (0.0)	-
Pons	1 (5.6)	3 (16.7)	0.603
Medulla oblongata	1 (5.6)	4 (22.2)	0.338
Cerebellum	4 (22.2)	1 (5.6)	0.338
Multifocal lesions	3 (16.7)	0 (0.0)	0.229
Bilateral lesions at CR/BG/IC	4 (22.2)	9 (50.0)	0.164
Severe white matter hyperintensities	1 (5.6)	6 (33.3)	0.088
Clinical dysphagia scale≥20	7 (38.9)	11 (61.1)	0.182
Initial tube feeding	1 (5.6)	14 (77.8)	<0.001*

BG, basal ganglia; CR, corona radiata; IC, internal capsule; NIHSS, National Institutes of Health Stroke Scale.

*P-value<0.05.

3.2.2. Functional Regression Analysis for Hyoid Displacement

Fig. 3.4 shows the mean two-dimensional trajectories of the hyoid bone during swallowing in the age- and sex-matched stroke patients with good and poor prognosis for swallowing function. The mean HDs in the horizontal and vertical planes for the two groups are shown in Fig. 3.5 (A, C). The regression coefficient functions representing intergroup differences for the horizontal and vertical HDs over time between the two groups are shown in Fig. 3.5 (B, D). Horizontal HD differed significantly between the patients with good and poor prognosis over the forward motions (35^{th}–78^{th} percentiles). Vertical HD showed significant difference over time between the two groups over the forward motions (9^{th}–32^{nd} percentiles).

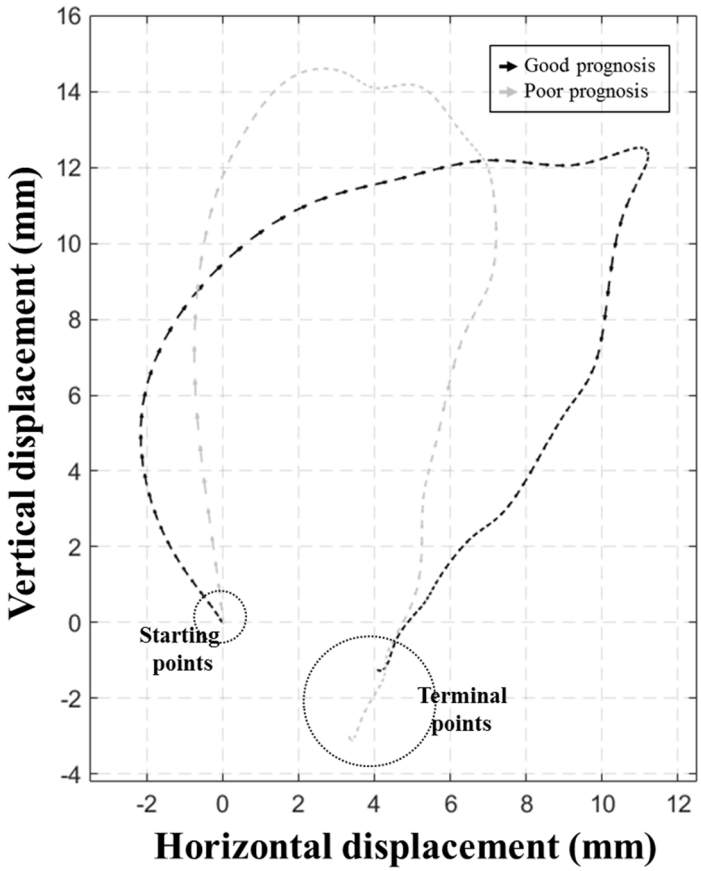

Fig. 3.4. The mean two-dimensional trajectories of the hyoid bone during swallowing in age- and sex-matched stroke patients with good and poor prognosis for swallowing function

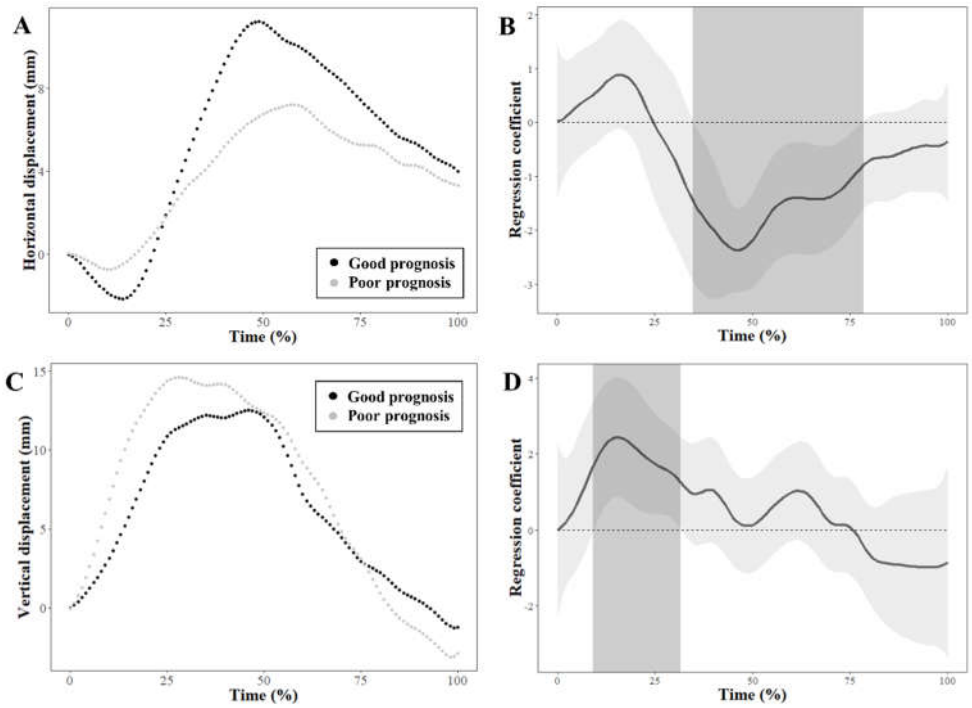

Fig. 3.5. Results of functional regression analysis for horizontal and vertical hyoid displacements. Mean trajectories are illustrated for the horizontal (A) and vertical (C) displacements in age- and sex-matched stroke patients with good and poor prognosis. Estimated regression coefficient functions with 95% confidence intervals are shown for the horizontal and vertical displacements between stroke patients with good and poor prognosis (B, D). The light gray zones denote the time interval where the mean difference is significant between the groups.

3.2.3. Functional Regression Analysis for Hyoid Velocity

The mean HVs in the horizontal and vertical planes for the age- and sex-matched stroke patients with good and poor prognosis for swallowing function are shown in Fig. 3.6 (A, C). The regression coefficient functions representing intergroup differences for the horizontal and vertical HVs over time between the two groups are shown in Fig. 3.6 (B, D). The HV showed significant differences between the patients with good and poor prognosis at the 28^{th}-36^{th}/51^{rd}-56^{th}/74^{th}-79^{th} percentiles in the horizontal plane, and the 5^{th}-11^{st}/44^{th}-45^{th} percentiles in the vertical plane.

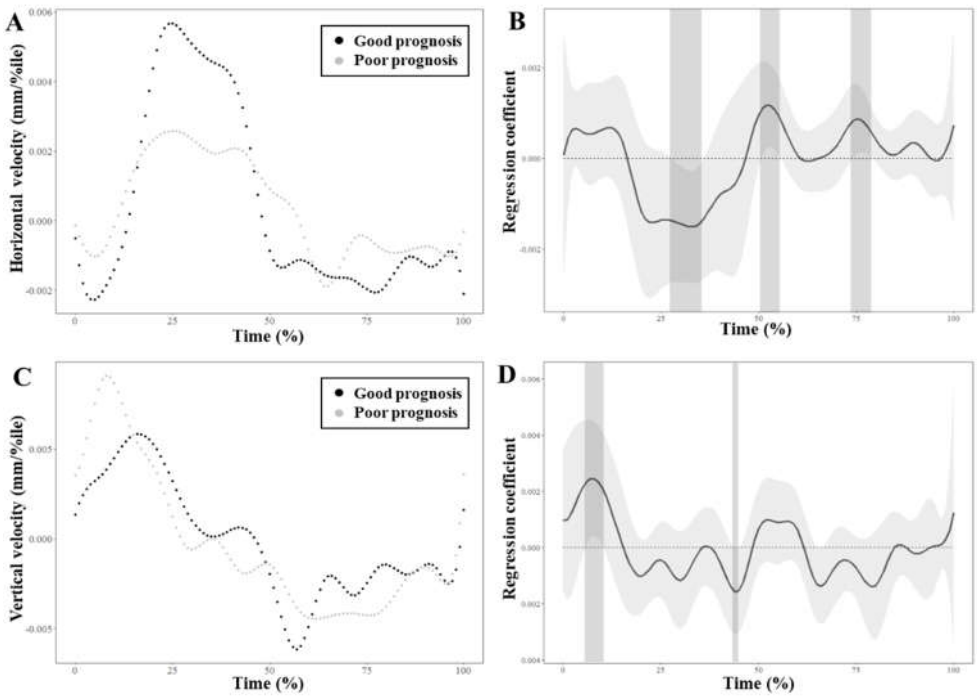

Fig. 3.6. Results of functional regression analysis for horizontal and vertical hyoid velocities. Mean trajectories are illustrated for the horizontal (A) and vertical (C) displacements in age- and sex-matched stroke patients with good and poor prognosis. Estimated regression coefficient functions with 95% confidence intervals are shown for the horizontal (B) and vertical (D) velocities between stroke patients with good and poor prognosis. The light gray zones denote the time interval where the mean difference is significant between the groups.

3.2.4. Functional Regression Analysis for Hyoid Direction Angle

The mean trajectories for the hyoid direction angles in the age- and sex-matched stroke patients with good and poor prognosis for swallowing function are illustrated in Fig. 3.7 (A). The regression coefficient function representing intergroup differences over time between the two groups is shown in Fig. 3.7 (B). The hyoid direction angle showed significant differences between the patients with good and poor prognosis at the 12^{nd}-19^{th}/76^{th}-99^{th} percentiles.

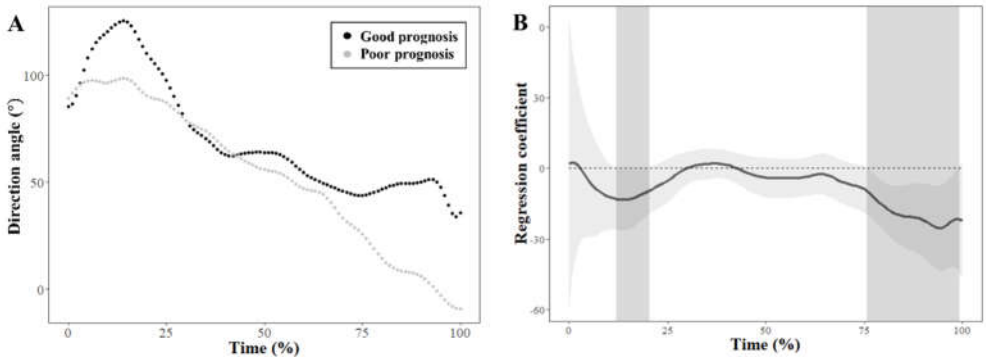

Fig. 3.7. Results of functional regression analysis for hyoid direction angles. Mean trajectories are illustrated for the direction angles in age- and sex-matched stroke patients with good and poor prognosis (A). Estimated regression coefficient functions with 95% confidence intervals are shown for the direction angles between stroke patients with good and poor prognosis (B). The light gray zones denote the time interval where the mean difference is significant between the groups.

3.2.5. Analysis for Maximal Values of Hyoid Kinematic Parameters

Table 3.10 shows the results of analysis for the maximal values of HD and HV, and mean direction angle for 5-20%ile duration. Both maximal horizontal HD (P=0.031) and HV (P=0.034) in the forward motions differed significantly between patients with the two groups. Mean direction angle for 5-20%ile duration was significantly different between the two groups (P=0.050).

Table 3.10. Results of analysis for the maximal and mean kinematic parameters of hyoid motion in age- and sex-matched stroke patients with good and poor prognosis

	Good prognosis (n=18)	Poor prognosis (n=18)	*P*
Maximal horizontal displacement (mm)			
Backward	-3.49±2.59	-3.01±3.36	0.282
Forward	12.43±4.81	9.22±3.95	0.031*
Maximal vertical displacement (mm)			
Upward	15.37±7.14	16.81±7.10	0.548
Time to maximal displacement (%ile)			
Horizontal, backward	17.38±7.45	17.14±14.53	0.950
Horizontal, forward	48.96±8.69	47.98±13.76	0.799
Vertical, upward	36.73±13.26	31.87±10.44	0.230
Maximal horizontal velocity (mm/%ile)			
Backward	-0.63±0.41	-0.56±0.38	0.393
Forward	1.28±0.50	0.96±0.43	0.034*
Maximal vertical velocity (mm/%ile)			
Upward	1.36±0.52	1.76±0.98	0.114
Time to maximal velocity (%ile)			
Horizontal, backward	25.36±22.24	16.02±17.60	0.173
Horizontal, forward	29.21±8.25	25.64±14.53	0.372
Vertical, upward	19.20±10.97	13.81±10.83	0.071
Mean direction angle for 5-20%ile duration	119.18±38.19	96.45±33.91	0.050*

Values are presented as mean ± standard deviation.

**P*-value<0.05.

3.3. Survival Analysis in Patients with Post-stroke Dysphagia

3.3.1. Clinical Characteristics

A total of 137 patients with acute ischemic stroke were included in this study. The information of demographic, neurologic, and swallowing characteristics is shown in Table 3.8. The mean age of the study group was 68.7 (±14.0) years and sixty-nine (50.4%) patients were males. The mean duration from stroke onset to initial VFSS was 16.8 (±8.3) days. Significant differences were observed between the patients with good (n=113, 82.5%) and poor (n=24, 17.5%) prognosis for variables including age ≥ 65 (P=0.023), male sex (P=0.008), anterolateral territory of brainstem (P=0.021), bilateral lesions at CR/BG/IC (P<0.001), severe WMH (P=0.011), CDS≥20 (P=0.001), and initial tube feeding (P<0.001). No significant difference was observed between each lesion location of patients with good and poor prognosis.

3.3.2. Survival Analysis

The Kaplan-Meier estimates indicated that the mean duration of swallowing recovery was 65.6 days (95% confidence interval [CI], 54.8–76.5), as shown in Fig. 3.8 (A). According to the subgroup analysis, the mean duration of the patients with good prognosis was 41.0 days (95% CI, 33.5–48.5). In log-rank test, the duration of swallowing recovery was significantly different depending on the covariates including initial tube feeding (P<0.001), CDS≥20 (P=0.001), male sex (P=0.010), bilateral lesions at CR/BG/IC (P<0.001), and severe WMH (P=0.010), which are shown in Fig. 3.8 (B-F). The results of univariable and multivariable Cox proportional-hazards models for the risk of poor swallowing recovery are shown in Table 3.11.

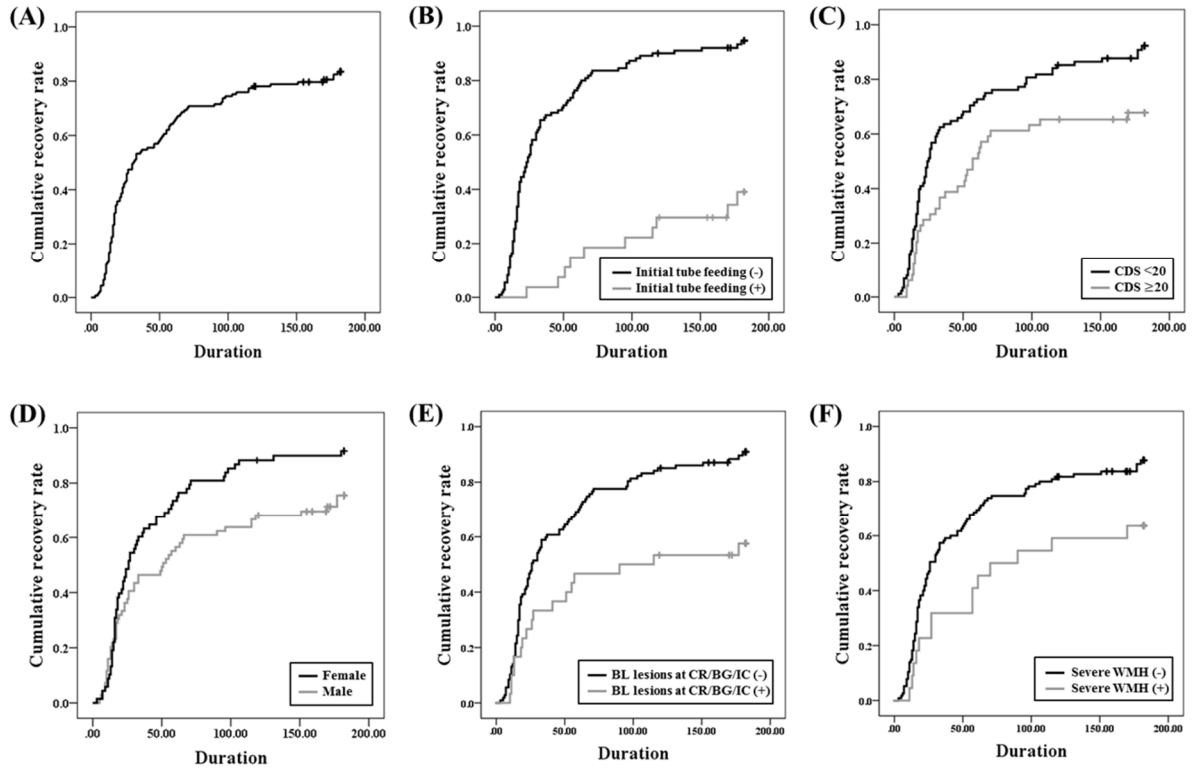

Fig. 3.8. Kaplan-Meier estimates in patients with post-stroke dysphagia for overall swallowing recovery (A) and swallowing recovery depending on the factors including initial tube feeding (B), clinical dysphagia scale (CDS) (C), sex (D), bilateral lesions at corona radiata, basal ganglia, and/or internal capsule (CR/BG/IC) (E), and severe white matter hyperintensities (F).

Table 3.11. Univariable and multivariable Cox proportional-hazards models for the risk of poor recovery of swallowing function

Variables	Univariable analysis		Multivariable analysis	
	Hazard ratio (95% CI)	*P*-value	Hazard ratio (95% CI)	*P*-value
Male sex	1.62 (1.12-2.37)	0.011*		
CR	1.46 (0.99-2.14)	0.056		
BG/IC	1.36 (0.93-1.99)	0.118		
Insula	1.47 (0.94-2.30)	0.088		
Lesion laterality	0.77 (0.56-1.05)	0.094		
Right	1.00	-		
Left	1.18 (0.63-2.21)	0.617		
Bilateral	0.70 (0.37-1.31)	0.257		
Anterolateral territory of brainstem	1.72 (0.80-3.71)	0.167		
Bilateral lesions at CR/BG/IC	2.46 (1.46-4.14)	0.001*	2.38 (1.41-4.03)	0.001*
Severe WMH	2.09 (1.21-3.61)	0.008*		
Clinical dysphagia scale≥20	1.94 (1.29-2.93)	0.001*	1.53 (1.02-2.31)	0.042*
Initial tube feeding	6.64 (3.42-2.87)	<0.001*	5.93 (3.04-11.57)	<0.001*

BG: basal ganglia; CI: confidence interval; CR: corona radiata; IC: internal capsule; WMH: white matter hyperintensities.

* *P*-value<0.05.

3.4. Development and Validation of Prognostic Models in Post-stroke Dysphagia

After recursive feature elimination (Fig. 3.9), twelve feature variables were selected in the prognostic models as follows: (i) initial tube feeding, (ii) bilateral lesions at CR/BG/IC, (iii) CDS $\geq$ 20, (iv) severe WMH, (v) lesions at CR, (vi) maximal horizontal backward displacement, (vii) maximal horizontal forward displacement, (viii) maximal vertical displacement, (ix) maximal vertical velocity, (x) time at maximal horizontal backward displacement, (xi) time at maximal vertical displacement, and (xii) mean direction angle for 5-20%ile duration. The results of performance evaluation for the prognostic models are shown in Table 3.12. In prediction of 6-month swallowing recovery, the classifier based on an XGBoost algorithm outperforms the other classifiers based on the benchmarking algorithms including support vector machine, random forest, and artificial neural networks with an area under the ROC curve of 0.881, F1 score of 0.945, and MCC of 0.718. Relative feature importance for each feature variable based on XGBoost were represented in Fig. 3.10. Top-5 important feature variables were as follows: (i) initial tube feeding, (ii) maximal vertical displacement, (iii) bilateral lesions at CR/BG/IC, (iv) mean direction angle for 5-20%ile duration, and (v) time at maximal vertical displacement.

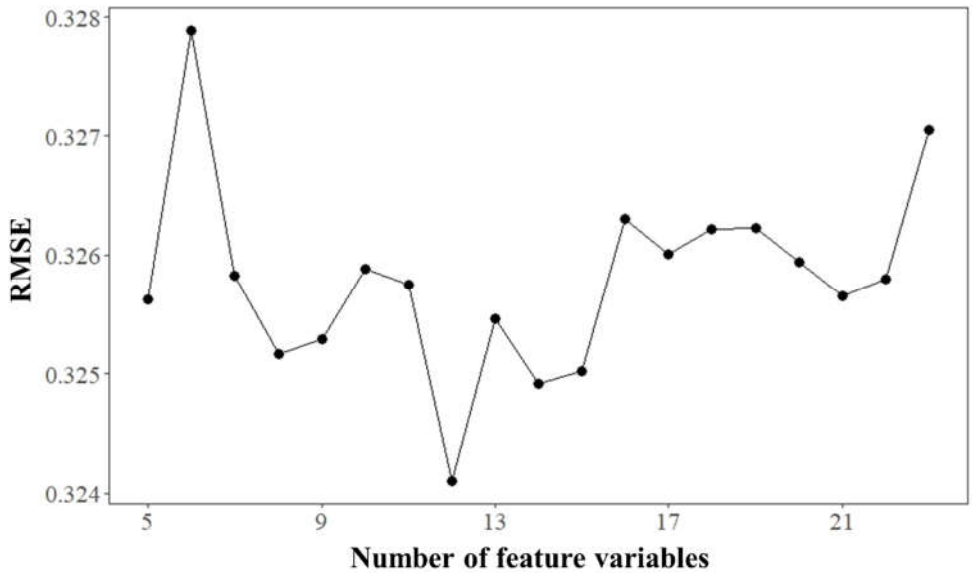

Fig. 3.9. Root mean squared error (RMSE) corresponding to the number of feature variables by a recursive feature elimination algorithm. RMSE is minimized with twelve feature variables.

Table 3.12. The results of performance evaluation for the prediction models

	Extreme gradient boosting	Artificial neural networks	Random forest	Support vector machine
AUC	0.881	0.814	0.798	0.839
F1 score	0.945	0.947	0.929	0.809
Matthews correlation coefficient	0.718	0.679	0.595	0.521

AUC: area under the receiver operating characteristic curve

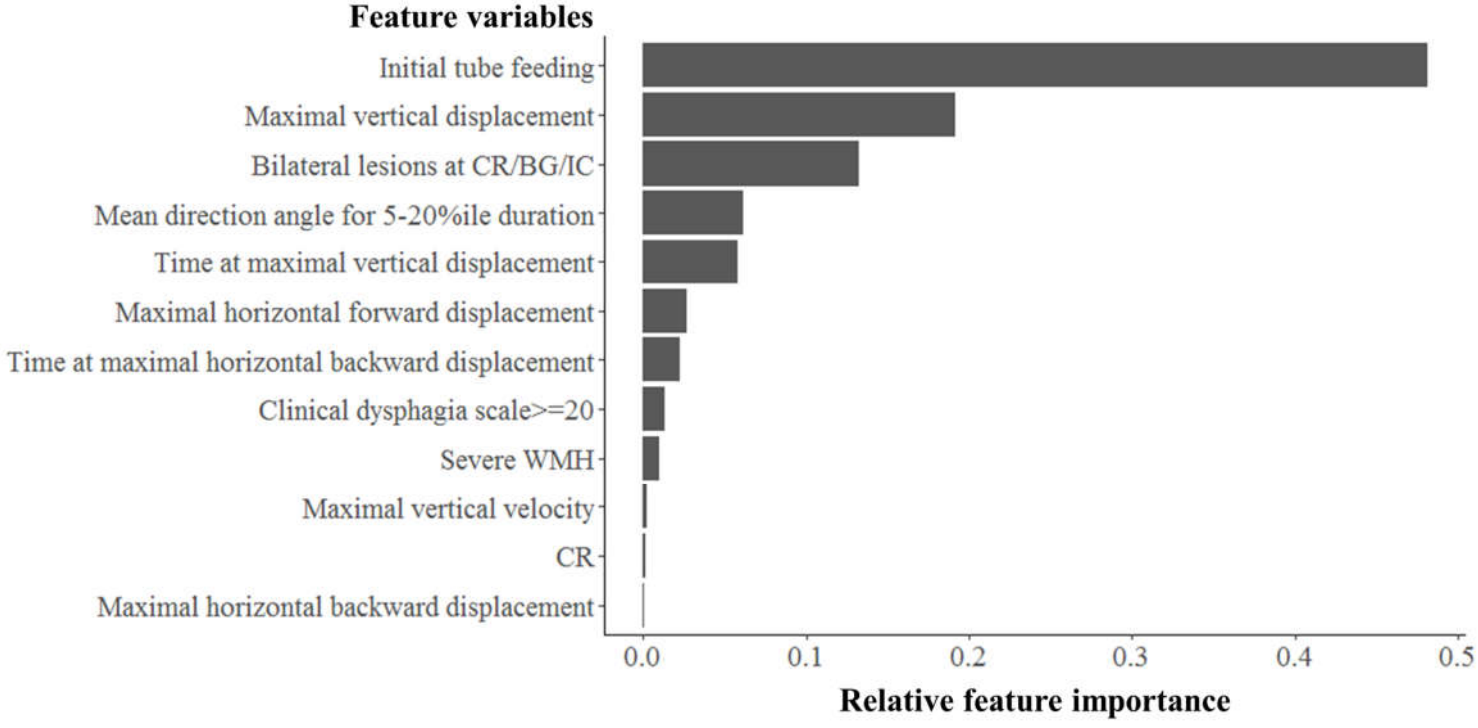

Fig. 3.10. Feature importance for selected twelve kinematic, clinical, and radiologic variables using an extreme gradient boosting algorithm.

4. Discussion

4.1. Differential Kinematic Features in Patients with Parkinson's Disease and Ischemic Stroke

To the best of our knowledge, this is the first study to specifically assess pointwise differences in swallowing motion over time in patients with brain disorders. Traditional approaches for the analysis of swallowing motion involve comparison of mean or maximal values over the time course of the observational data.[75] Maximal and mean values of HD and HV have been reported to be significant parameters to differentiate patients with dysphagia from healthy controls, which was grossly consistent with the findings of the current study.[28,86,87] The present study revealed several novel features of the hyoid kinematics in dysphagia patients with brain disorders, by normalizing and transforming discrete data of hyoid motion to functional data. The analyses of maximal values for the kinematic parameters also showed consistent results with these findings.

The current study presents the kinematic features of swallowing in patients with PD and ischemic stroke using FLR. An analysis of the entire motion profiles of the hyoid bone during swallowing enabled sensitive detection of distinct features of swallowing in patients with dysphagia. In PD patients, horizontal HD and HV were decreased during the initial backward and forward motions, which was supported by the results of analysis of the maximal HD and HV between patients with PD and healthy elderly controls. The trajectories of the hyoid bone during swallowing in patients with PD could be distinguished from normal age-related changes by the

comparison between the healthy elderly and young controls. In patients with ischemic stroke, horizontal HD and HV during the forward motions and direction angle during the early phase of swallowing were reduced in patients with poor prognosis compared to those with good prognosis.

In PD patients, the VDS, which is the swallowing functional scale based on the VFSS, showed significant correlations with the horizontal HD and HV in the initial backward and forward motions. Patients with PD demonstrated significant reduction in maximal values of vertical HV despite preservation of vertical HD. Multiple swallowing parameters rated by the VDS showed a significant association with the horizontal HD and/or HV of the initial backward motion, including triggering of pharyngeal swallow, vallecular residue, laryngeal elevation, coating on the pharyngeal wall, pharyngeal transit time, and aspiration. Additionally, healthy elderly controls showed significantly decreased horizontal HD in forward motion, but increased vertical HD in upward motion compared to the healthy young controls in FLR, even though no significant difference was observed in the maximal values of HD. These results indicated that reduced horizontal displacement and velocity of the hyoid bone over the forward motion during swallowing could be attributed to the combined effects of disease and aging, whereas those over the initial backward motion can be considered specific to patients with PD.

In the present study, hyoid motion of the early phase of swallowing was investigated in PD patients and ischemic stroke. The backward motion of the hyoid bone was preserved regardless of aging, which implies that reduced backward motion of the hyoid bone during the early phase of swallowing may be one of the pathologic findings in PD patients with dysphagia. Likewise, direction angle during the initial phase of swallowing was decreased in stroke patients with poor prognosis

compared to those with good prognosis, which can be in line with the results of the kinematic studies for PD patients. In fact, few studies have been published on the physiological role of initial backward hyoid motion on swallowing function. According to the literature, the suprahyoid muscles were sequentially recruited during swallowing by contractions of the stylohyoid, posterior digastric, and mylohyoid muscles, followed by those of the geniohyoid and anterior digastric muscles.[25,88] In the activation sequences, the stylohyoid and posterior digastric muscles with the force vector in the backward-upward direction can have the capacity to pull the hyoid bone backward simultaneously or prior to moving it in forward-upward direction.[89] If the backward and forward motions of the hyoid bone are sequentially engaged in the initial swallowing process, it might be assumed that the backward motion helps generate strong forces for the forward/upward motion by increasing the length of the suprahyoid muscles in the early phase of swallowing.[90] The biomechanics of pulling the hyoid bone forward by the suprahyoid muscles, which behave with viscoelastic properties, can be possibly impaired in individuals with a reduced backward motion of the hyoid bone.[91,92] The sequential activation of the suprahyoid muscles can be affected by primary motor manifestations including resting tremor, bradykinesia, incoordination, and rigidity in PD patients or disruption of brain networks associated with muscle activity for swallowing in stroke patients. These can plausibly underlie the altered hyoid kinematics, resulting in impaired safety and efficacy of swallowing. Further studies are necessary to elucidate detailed biomechanical properties and physiological role of the hyoid motion during initial phase of swallowing in patients with PD and ischemic stroke.

Interestingly, maximal vertical HD was not different significantly between PD patients and healthy controls, which was consistent with the results of previous

studies.[28,93] In stroke patients, vertical HD was even higher during swallowing process in patients with poor prognosis than those with good prognosis, even though maximal vertical HD was not different significantly between the two groups. Vertical HD was preserved or even exaggerated in aging and brain disorders such as PD and stroke, which is the distinct results from the horizontal HD.[93] One hypothesis to account for the abnormal swallowing pattern is a compensatory response by the remaining functions of swallowing-related neuromuscular structures. Since swallowing is controlled by both sides of the brain asymmetrically, compensation from the undamaged brain might be represented as increased vertical HD and HV in stroke patients.[94,95] Moreover, a previous study demonstrated that effortful swallowing, which is regarded as an important compensatory mechanism in dysphagia, leads to increase every parameter of maximal displacement and velocity of the hyolaryngeal complex except the horizontal HD and HV, which is consistent with the results of the current study.[96] Additional biomechanical study of the individual hyoid muscles is required to prove the compensatory mechanisms in aging and patients with PD and stroke.

4.2. Functional Data Analysis

Functional data analysis is a statistical method for analyzing functional data and can be applied to noise reduction, derivative calculation, and fitting parameters of dynamic systems. This method can be a preliminarily approach for more structured analyses and for providing novel insights into hidden mechanisms.[75] Functional data analysis extends the capabilities of conventional analysis to capture the temporal patterns of time-series data and facilitates clear interpretation of changes in the shape of the curve.[31,75] In the present study, FLR, which is a part of functional data analysis, was successfully applied for observation of swallowing motions. The displacement and velocity, which are the main parameters of swallowing motion, are continuous, smooth, interrelated, and change over time. These properties meet the assumptions of functional data analysis, making it a powerful tool for analysis of the hyoid kinematics during swallowing. The results of the present study clarified the aspects that are important for differentiating dysphagia from normal swallowing functions. Since swallowing is a complex activity involving sequential interactions among bone, cartilage, muscle, and other structures, these aspects would be critical to demonstrate differences in motions between patients with and without dysphagia or with good and poor prognosis.

4.3. Clinical and Radiologic Factors Associated with Long-term Swallowing Recovery

The current study aimed to identify the clinical and radiologic factors of swallowing function in patients with post-stroke dysphagia and develop prognostic models in order to predict its long-term prognosis using the relevant factors. The results of the survival analysis indicated that the 6-month swallowing recovery after stroke differed significantly depending on clinical (initial tube feeding, CDS, and male sex) and radiologic factors (bilateral lesions at CR/BG/IC and severe WMH). Particularly, bilateral lesions at CR/BG/IC were newly reported as a significant prognostic factor of post-stroke dysphagia in this study.

Initial dysphagia severity was the most significant prognostic factor for long-term recovery of swallowing function in the present study. This finding is not surprising given that initial dysphagia severity can reflect the degree of initial neurologic injury specific to swallowing function. Initial dysphagia severity has been regarded as the most significant prognostic factors for both short- and long-term recovery in the previous studies.[39,54,59,60,97,98] On the other hand, initial stroke severity, measured with NIHSS did not show any significant association with long-term recovery of swallowing function. In fact, NIHSS have shown inconsistent results for even short-term (<1 month) swallowing recovery.[39,52,54] Considering that NIHSS is one of the most important prognostic factor for functional recovery after stroke, prognosis of swallowing recovery needs to be considered separately.[67]

Interestingly, the bilateral lesions at CR/BG/IC was one of the significant factors associated with poor recovery of swallowing function in this study. Although the old lesions of the contralesional side have not been noted as one of the candidates

for prognostic factors, previous studies have investigated the risk of bilateral brain injury on swallowing recovery.[52,54,60] In swallowing physiology, swallowing is regulated by brain in a bilateral, but asymmetric manner, which induces great variability of representation of swallowing impairment in patients with unilateral stroke.[94] Bilateral stroke can lead deterioration of swallowing recovery since it may diminish compensatory reorganization from undamaged brain.[95] The current study presents the necessity to add the old lesions of CR/BG/IC at the contralesional side as an important prognostic factor even if the old lesions did not cause any neurologic symptom or sequelae. Functional representation masked by compensation of the unaffected brain might be deteriorated with subsequent insults at contralateral brain regions. Foix-Chavany-Marie syndrome, which is also called opercular syndrome, were reported to cause severe dysphagia.[99–102] It can be represented in a variety of lesion locations including bilateral opercular infarcts, operculum and CR at each side, and bilateral CR.[100] Old infarcts followed by new insults on the brain could result in severe dysfunction and poor recovery of swallowing.[99,100] Plausible hypothesis is that severe pharyngeal paralysis occur due to bilateral disruption of corticobulbar tracts to the ambiguous and the hypoglossal nuclei involving cranial nerves 9, 10, and 12.[99,101] Additionally, bilateral lacunar infarcts at BG or subcortical white matter can cause vascular Parkinsonism, which can be related with post-stroke dysphagia and poor recovery of swallowing function.[103,104] The neuroimaging researches based on tractography or metabolic activity are warranted to investigate the relationship between injury severity of bilateral corticobulbar tracts or basal ganglia and their changes during swallowing recovery.

Recently, cerebral small vessel disease has been getting great interest with increasing elderly population and advance in cerebral imaging.[105] It develops in

accordance with cumulated injuries of cerebral microvascular beds over time and causes negative impacts on stroke occurrence and recovery.[106,107] WMH, which is one of the neuroimaging features of small vessel disease, was the significant independent factor affecting swallowing recovery until 6 months in the Cox proportional-hazards model. Previously, the impact of WMH on swallowing function has been investigated only for short-term (9.5 days in average) swallowing recovery after stroke.[55] This study showed severity of WMH in older patients with mild stroke is associated with swallowing impairment such as prolonged oral transit time and increased penetration. The present study revealed that severe WMH can also affect long-term swallowing recovery for 6 months after stroke. In previous literature, coexisting cerebral small vessel disease including WMH can deteriorate functional and cognitive outcomes after stroke.[106] Rapid deterioration of cognitive impairments caused by ischemic stroke predisposing severe WMH can exacerbate oral phase dysphagia and attenuate active participation in swallowing rehabilitation during the time windows for neuroplasticity.[106] The pathological process to deteriorate functional recovery of swallowing should be elucidated in further study.

4.4. Machine Learning-based Prognostic Models for Long-term Swallowing Recovery

An XGBoost model to predict long-term swallowing recovery after ischemic stroke was developed by selecting the feature variables based on the survival analyses, which resulted in the achievement of the prediction performance with ROC curve of 0.81. ADASYN, which is one of the class rebalancing techniques, led to improve the prediction performance by alleviating class imbalance between the patients with good and poor prognosis. An area under the ROC curve, F1 score, and MCC showed good discrimination. In addition to the prediction performance, good interpretability of the XGBoost model has great strength for decision making in medicine where errors can have a dire consequence.[108] In this study, the XGBoost model intuitively showed the importance of feature variables. Top-5 important feature variables include three kinematic variables (value and time of maximal vertical displacement and mean direction angle for 5-20%ile duration), one clinical variable (initial tube feeding), and one radiologic variable (bilateral lesions at CR/BG/IC).

In clinical point of view, the prognostic model for 6-month swallowing recovery can be beneficial for planning of tube removal, scheduling reevaluations, and counseling for patient and their families in post-stroke care by individualizing long-term recovery trajectories.[49] For patients with gastrostomy tube who are classified as good prognosis (recovering to nearly pre-stroke status before 6 months) according to this model, interval for reevaluations can be reduced to remove gastrostomy tube compared to those classified as poor prognosis. This can alleviate unnecessary restraint of oral intake that can interfere improvement of swallowing function after stroke. In addition, if the patients who needs only diet modification are classified as poor prognosis (persisting until 6 months) based on the developed

model, it can be needed to not only provide education for modification of diets (foods and beverages), but also enhance its compliance of the patients and their families for keeping diet modification strictly to prevent aspiration pneumonia. Clinically, poor compliance for the diet modification due to low quality of life can induce silent aspiration particularly in elderly patients, which results in life-threatening pneumonia. As such, development of long-term prognostic model for swallowing recovery using machine learning algorithms can be a meaningful approach by providing useful information in patient care and planning.

Prognostic models for post-stroke dysphagia have been developed to predict the feeding status that requires tube placement in previous studies. Dubin et al. developed prognostic models to predict feeding via gastrostomy tube based on the logistic regression using variables known by 24 hours from admission including age≥80, NIHSS 8-14 (and >14), the African race, and infarct location involving the cortex.[51] More robust prognostic models were established on the prospective cohorts by Galovic et al. to predict the recovery of oral intake and return to pre-stroke diet on day 7 and 30.[39] Five factors including age≥70, NIHSS at admission, lesion of the frontal operculum, initial risk of aspiration, and initial score of functional oral intake scale were selected to develop the prognostic score system with external multicenter validation. In the present study, the XGBoost-based prognostic model was developed utilizing kinematic, clinical, and radiologic factors to predict 6-month swallowing recovery. Since the majority of spontaneous recovery occurs within the first 6 months after stroke, it can be the primary endpoint of persistent dysphagia in patients with ischemic stroke and used as the clinical outcome in this study.[109,110] The prediction of short- and long-term swallowing recovery can be complemented by the prognostic models from previous and current studies and may contribute to optimize dysphagia evaluation, management, and education for individuals with ischemic stroke.

4.5. Limitations

This study has several limitations. For the kinematic analysis for PD and ischemic stroke patients, first, the liquid volume provided for patients who were included in the analysis was only 2 ml. In fact, larger volume than 2ml of the diluted barium solution was not tried for some of the dysphagia patients who showed deep penetration or aspiration of 2ml liquid during examination. VFSS was performed with priority for the comprehensive evaluation and patient safety in the tertiary hospital. Interestingly, particularly for PD patients, a previous study reported that a distinct pattern of changes in hyoid motion was not observed with respect to bolus volume in contrast with healthy adults.[111] This study interpreted that hypokinesia in PD patients was represented as lack of adaptation for the larger bolus. Further studies are necessary to investigate the volume effect on hyoid kinematics in PD patients. Second, time delay from intention to swallowing behavior or absolute velocity of the hyoid motion was not analyzed in this study. The normalized profiles of spatiotemporal data are not for the food bolus, but for the hyoid motion per se. Third, the sample size was relatively small. Further research should be supported by a large population of PD and ischemic stroke patients. Fourth, impairment severity for the general physical function in PD patients including the Hoehn and Yahr stage was not measured due to retrospective nature of the study. However, the severity of dysphagia of all patients with PD included in the present study was measured using the ASHA-NOMS swallowing scale, and only cases of mild to moderate dysphagia with ratings of 5-6 were included.

For the study of survival analysis and prognostic model development for ischemic stroke patients, first, the class was imbalanced and the sample size was small, particularly for the patients with poor prognosis. To overcome these issues,

ADASYN was used to synthesize data in poor prognosis and rebalance proportion of the class, which could improve the classification performance. Cross-validation was conducted during oversampling to avoid overfitting and over-optimistic estimates. The developed model was evaluated using the only test set that was not contaminated with the training set. Second, the data collection was conducted retrospectively. However, the missing data was nearly none for all variables, except for the NIHSS score of four patients. To consider the development of classification model, patients without information of swallowing function for a period longer than 4 months after the stroke were excluded. Third, the retrospective cohorts of the present study may not include ischemic stroke patients with very mild or very severe dysphagia who were not required or unable to undergo VFSS. Those can represent patients with post-stroke dysphagia who are needed to be evaluated for swallowing function in general clinical practice. Fourth, external validation was not performed in this study. Future study is needed to include model validation for datasets from other independent institutions. Fifth, vertical displacement and velocity of the hyoid bone, which are the important kinematic factors in the prognostic model, might negatively impact on its classification performance for patients with severe pharyngeal weakness in whom the compensatory mechanism can even be damaged.

5. Concluding Remarks and Future Work

The present study revealed the differential kinematic features of swallowing in patients with PD and ischemic stroke. In PD patients, reduced horizontal HD and HV during the initial backward and forward motions are important kinematic features of swallowing. The reduced horizontal displacement and velocity of the hyoid bone over the forward motion could be attributed to the combined effects of disease and aging, whereas those over the initial backward motion may be considered specific to patients with PD. The results implicated that horizontal HD and HV during the initial backward and forward motions can have potential clinical usefulness to estimate the swallowing impairment in PD patients. In ischemic stroke patients, reduced horizontal HD and HV during the forward motion and decreased mean direction angle during initial phase of swallowing are important kinematic features of swallowing in patients with poor prognosis of swallowing recovery. Initial backward motion as well as horizontal forward motion is critical to differentiate the ischemic stroke patients with good and poor prognosis, which can be in line with the results of investigation for PD patients. It can be characteristic that the hyoid motion during early phase of swallowing is associated with the severity or prognosis of dysphagia. Future study is warranted to investigate biomechanical aspects of initial hyoid motion considering viscoelastic properties of the supra- and infrahyoid muscles and its physiological role for pharyngeal passages and protecting aspiration during swallowing. Additionally, effect of volume and viscosity for food bolus on hyoid motion should be additionally investigated in regarding to the initial motion of hyoid bone and severity or prognosis of dysphagia.

In order to predict long-term swallowing recovery, initial dysphagia severity and bilateral lesions at CR/BG/IC were the significant clinical and radiologic factors associated with 6-month swallowing recovery, respectively. Particularly, the current study presents the need to assess old lesions of CR/BG/IC at the contralesional side, even if those did not cause any neurologic symptom or sequelae following the previous stroke. Because there has been still a paucity for physiological effect of the bilateral subcortical disruptions on swallowing function or recovery, neuroimaging investigations based on tractography or metabolic activity are needed in further studies. Prediction of 6-month swallowing recovery in post-stroke dysphagia was feasible using the proposed XGBoost model based on the kinematic, clinical and radiologic factors. In clinical point of view, the prognostic model for 6-month swallowing recovery can be beneficial for management and planning in post-stroke care by individualizing long-term recovery trajectories. This study emphasizes that initial backward motions of the hyoid bone and bilateral subcortical lesions are important prognostic factors and can be utilized to develop prognostic models for long-term swallowing recovery in ischemic stroke. Future study is necessary to perform external validation for developing robust and generalizable prognostic models. Additionally, since the kinematic parameters are acquired by manual marking which needs labor-intensive and time-consuming works, further study is warranted to add functionality of automatic hyoid bone tracking for clinical utility of the developed prognostic model.

Acknowledgments

Parts of this thesis were published in the ***Journal of Electromyography and Kinesiology*** and ***Stroke***:

1. Lee WH, Lim MH, Nam HS, Kim YJ, Seo HG, Bang MS, Seong MY, Oh BM, and Kim SW. Differential kinematic features of the hyoid bone during swallowing in patients with Parkinson's disease. *J. Electromyogr. Kinesiol.* 2019. 47, 57–64. doi: 10.1016/j.jelekin.2019.05.011

2. Lee WH, Lim MH, Seong MY, Seo HG, Oh BM, and Kim SW. Development of a novel prognostic model to predict 6-month swallowing recovery after ischemic stroke. *Stroke*. In press. doi: 10.1161/STROKEAHA.119.027439

Funding

This study was supported by grant No. 0420170660 from the SNUH Research Fund.

References

1. Davie CA. A review of Parkinson's disease. *Br Med Bull*. 2008;86(1):109-127.

2. Daniels SK, Brailey K, Priestly DH, Herrington LR, Weisberg LA, Foundas AL. Aspiration in patients with acute stroke. *Arch Phys Med Rehabil*. 1998;79(1):14-19.

3. Mackay LE, Morgan AS, Bernstein BA. Swallowing disorders in severe brain injury: risk factors affecting return to oral intake. *Arch Phys Med Rehabil*. 1999;80(4):365-371.

4. Winstein CJ. Neurogenic dysphagia. Frequency, progression, and outcome in adults following head injury. *Phys Ther*. 1983;63(12):1992-1997.

5. Horner J, Alberts MJ, Dawson D V, Cook GM. Swallowing in Alzheimer's disease. *Alzheimer Dis Assoc Disord*. 1994;8(3):177-189.

6. Volicer L, Seltzer B, Rheaume Y, et al. Eating difficulties in patients with probable dementia of the Alzheimer type. *J Geriatr Psychiatry Neurol*. 1989;2(4):188-195.

7. Wirth R, Dziewas R, Beck AM, et al. Oropharyngeal dysphagia in older persons – from pathophysiology to adequate intervention: A review and summary of an international expert meeting. *Clin Interv Aging*. 2016;11:189-208.

8. Schindler JS, Kelly JH. Swallowing disorders in the elderly. *Laryngoscope*. 2002;112(4):589-602.

9. Mann G, Hankey GJ, Cameron D. Swallowing function after stroke: prognosis and prognostic factors at 6 months. *Stroke*. 2011;30(4):744-748.

10. Vesey S. Dysphagia and quality of life. *Br J Community Nurs*. 2014;18(Sup5):S14-S19.

11. Rofes L, Muriana D, Palomeras E, et al. Prevalence, risk factors and complications of oropharyngeal dysphagia in stroke patients: A cohort study. *Neurogastroenterol Motil*. 2018;30(8):1-10.

12. Miller N, Noble E, Jones D, Burn D. Hard to swallow: dysphagia in Parkinson's disease. *Age Ageing*. 2006;35(6):614-618.

13. Volonte MA, Porta M, Comi G. Clinical assessment of dysphagia in early phases of Parkinson's disease. *Neurol Sci*. 2002;23(SUPPL. 2):S121-S122.

14. Volonte MA, Porta M, Comi G, M.A. V, M. P, G. C. Clinical assessment of dysphagia in early phases of Parkinson's disease. *Neurol Sci*. 2002;23(SUPPL. 2):S121-S122.

15. Suttrup I, Warnecke T. Dysphagia in Parkinson's disease. *Dysphagia*. 2016;31(1):24-32.

16. Smithard DG. Long-term outcome after stroke : does dysphagia matter ? 2007:90-94.

17. Hamdy S, Aziz Q, Rothwell JC, et al. The cortical topography of human swallowing musculature in health and disease. *Nat Med*. 1996;2(11):1217-1224.

18. Singh S, Hamdy S. Dysphagia in stroke patients. *Postgrad Med J*. 2006;82:383-391.

19. Smithard DG, Neill PAO, England RE, et al. The Natural history of dysphagia following a stroke. 2014;193(February):188-193.

20. Feng X, Todd T, Hu Y, et al. Age-related changes of hyoid bone position in healthy older adults with aspiration. *Laryngoscope*. 2014;124(6).

21. Nam HS, Oh BM, Han TR. Temporal characteristics of hyolaryngeal structural movements in normal swallowing. *Laryngoscope*. 2015;125(9):2129-2133.

22. Ragland MC, Park T, Mccullough G, Kim Y. The speed of the hyoid excursion in normal swallowing. *Clin Arch Commun Disord*. 2016;1(1):30-35.

23. Dewan K, Chhetri DK. Epiglottic Dysfunction. In: *Dysphagia Evaluation and Management in Otolaryngology*. Elsevier; 2019:123.

24. Lee T, Park JH, Sohn C, et al. Failed deglutitive upper esophageal sphincter relaxation is a risk factor for aspiration in stroke patients with oropharyngeal dysphagia. *J Neurogastroenterol Motil*. 2017;23(1):34-40.

25. Okada T, Aoyagi Y, Inamoto Y, et al. Dynamic change in hyoid muscle length associated with trajectory of hyoid bone during swallowing: analysis using 320-row area detector computed tomography. *J Appl Physiol*. 2013;115(8):1138-1145.

26. Steele CM, Bailey GL, Chau T, et al. The relationship between hyoid and laryngeal displacement and swallowing impairment. *Clin Otolaryngol*. 2011;36(1):30-36.

27. Dodrill P, Gosa MM. Pediatric dysphagia: Physiology, assessment, and

management. *Ann Nutr Metab*. 2015;66:24-31.

28. Kim YH, Oh BM, Jung IY, Lee JC, Lee GJ, Han TR. Spatiotemporal characteristics of swallowing in Parkinson's disease. *Laryngoscope*. 2015;125(2):389-395.

29. Seo HG, Oh B, Han TR. Longitudinal changes of the swallowing process in subacute stroke patients with aspiration. 2011:41-48.

30. Seo HG, Oh B, Han TR. Swallowing kinematics and factors associated with laryngeal penetration and aspiration in stroke survivors with dysphagia. *Dysphagia*. 2016;31(2):160-168.

31. Durá J V., Belda JM, Poveda R, et al. Comparison of functional regression and nonfunctional regression approaches to the study of the walking velocity effect in force platform measures. *J Appl Biomech*. 2010;26(2):234-239.

32. Pearson WG, Langmore SE, Zumwalt AC. Evaluating the structural properties of suprahyoid muscles and their potential for moving the hyoid. *Dysphagia*. 2011;26(4):345-351.

33. Wang J-L, Chiou J-M, M¨uller H-G. Review of functional data analysis. *Annu Rev Stat Its Appl*. 2015;3:257-295.

34. Ullah S, Finch CF. Applications of functional data analysis: A systematic review. *BMC Med Res Methodol*. 2013;13:43.

35. Morris JS. Functional regression. *Annu Rev Stat Its Appl*. 2015;2:321-359.

36. Krekeler BN, Broadfoot CK, Johnson S, Connor NP, Rogus-Pulia N. Patient adherence to dysphagia recommendations: A systematic review. *Dysphagia*. 2018;33(2):173-184.

37. Balou M, Herzberg EG, Kamelhar D, Molfenter SM. An intensive swallowing exercise protocol for improving swallowing physiology in older adults with radiographically confirmed dysphagia. *Clin Interv Aging*. 2019;14:283-288.

38. George BP, Kelly AG, Schneider EB, Holloway RG. Current practices in feeding tube placement for US acute ischemic stroke inpatients. *Neurology*. 2014;83(10):874-882.

39. Galovic M, Stauber AJ, Leisi N, et al. Development and validation of a prognostic model of swallowing recovery and enteral tube feeding after ischemic stroke. *JAMA Neurol*. 2019;76(5):561-570.

40. Wirth R, Smoliner C, Jäger M, et al. Guideline clinical nutrition in patients

with stroke. *Exp Transl Stroke Med*. 2013;5(1):1-11.

41. Zhang Z, Coyle JL, Sejdić E. Automatic hyoid bone detection in fluoroscopic images using deep learning. *Sci Rep*. 2018;8(1):1-9.

42. Dudik JM, Coyle JL, El-Jaroudi A, Mao ZH, Sun M, Sejdić E. Deep learning for classification of normal swallows in adults. *Neurocomputing*. 2018;285:1-9.

43. Lopez-Meyer P, Makeyev O, Schuckers S, Melanson EL, Neuman MR, Sazonov E. Detection of food intake from swallowing sequences by supervised and unsupervised methods. *Ann Biomed Eng*. 2010;38(8):2766-2774.

44. Kodama C, Kato K, Tamura S, Hayamizu S. Swallowing function evaluation using deep-learning-based acoustic signal processing. *Proc - 9th Asia-Pacific Signal Inf Process Assoc Annu Summit Conf APSIPA ASC 2017*. 2018;2018-Febru(December):961-964.

45. Su C, Gao Y, Xie Y, Xue Y, Ge L, Li H. A hybrid classifier based on nonlinear-PCA and deep belief networks with applications in dysphagia diagnosis. *Comput Assist Surg*. 2017;22(0):135-147.

46. Lee J, Blain S, Casas M, Kenny D, Berall G, Chau T. A radial basis classifier for the automatic detection of aspiration in children with dysphagia. *J Neuroeng Rehabil*. 2006;3:1-17.

47. Kritas S, Dejaeger E, Tack J, Omari T, Rommel N. Objective prediction of pharyngeal swallow dysfunction in dysphagia through artificial neural network modeling. *Neurogastroenterol Motil*. 2016;28(3):336-344.

48. Lee JC, Seo HG, Lee WH, Kim HC, Han TR, Oh BM. Computer-assisted detection of swallowing difficulty. *Comput Methods Programs Biomed*. 2016;134(September 2013):79-88.

49. Wilmskoetter J, Herbert TL, Bonilha HS. Factors Associated with Gastrostomy Tube Removal in Patients with Dysphagia after Stroke. *Nutr Clin Pract*. 2017;32(2):166-174.

50. Jampathong N, Laopaiboon M, Rattanakanokchai S, Pattanittum P. Prognostic models for complete recovery in ischemic stroke: A systematic review and meta-analysis. *BMC Neurol*. 2018;18(1):1-11.

51. Dubin PH, Boehme AK, Siegler JE, et al. New model for predicting surgical feeding tube placement in patients with an acute stroke event. *Stroke*. 2013;44(11):3232-3234.

52. Kumar S, Langmore S, Goddeau RP, et al. Predictors of percutaneous

endoscopic gastrostomy tube placement in patients with severe dysphagia from an acute-subacute hemispheric infarction. *J Stroke Cerebrovasc Dis*. 2012;21(2):114-120.

53. Broadley S, Mbbs DC, Bapsc JC, Creevy M. Predictors of prolonged dysphagia following acute stroke. *J Clin Neurosci*. 2003;10(3):300-305.

54. Kumar S, Doughty C, Doros G, et al. Recovery of swallowing after dysphagic stroke: An analysis of prognostic factors. *J Stroke Cerebrovasc Dis*. 2014;23(1):56-62.

55. Moon HI, Nam JS, Leem MJ, Kim KH. Periventricular white matter lesions as a prognostic factor of swallowing function in older patients with mild stroke. *Dysphagia*. 2017;32(4):480-486.

56. Galovic M, Leisi N, Müller M, et al. Lesion location predicts transient and extended risk of aspiration after supratentorial ischemic stroke. *Stroke*. 2013;44(10):2760-2767.

57. Galovic M, Leisi N, Pastore-Wapp M, et al. Diverging lesion and connectivity patterns influence early and late swallowing recovery after hemispheric stroke. *Hum Brain Mapp*. 2017;38(4):2165-2176.

58. Steinhagen V, Grossmann A, Benecke R, Walter U. Swallowing disturbance pattern relates to brain lesion location in acute stroke patients. *Stroke*. 2009;40(5):1903-1906.

59. Schroeder MF, Daniels SK, McClain M, Corey DM, Foundas AL. Clinical and cognitive predictors of swallowing recovery in stroke. *J Rehabil Res Dev*. 2006;43(3):301.

60. Ickenstein GW, Kelly PJ, Furie KL, et al. Predictors of feeding gastrostomy tube removal in stroke patients with dysphagia. *J Stroke Cerebrovasc Dis*. 2003;12(4):169-174.

61. Kim J, Oh BM, Kim JY, Lee GJ, Lee SA, Han TR. Validation of the videofluoroscopic dysphagia scale in various etiologies. *Dysphagia*. 2014;29(4):438-443.

62. Leigh JH, Oh BM, Seo HG, et al. Influence of the chin-down and chin-tuck maneuver on the swallowing kinematics of healthy adults. *Dysphagia*. 2015;30(1):89-98.

63. Seong MY, Oh BM, Seo HG, Han TR. Influence of supraglottic swallow on swallowing kinematics: comparison between the young and the elderly. *J Korean Dysphagia Soc*. 2018;101(03080):23-29.

64. Kim K, Lee HS, Jung YH, et al. Mechanism of medullary infarction based

on arterial territory involvement. *J Clin Neurol*. 2012;8(2):116-122.

65. Kumral E, Bayülkem G, Evyapan D. Clinical spectrum of pontine infarction: Clinical-MRI correlations. *J Neurol*. 2002;249(12):1659-1670.

66. Chun SW, Lee SA, Jung I-Y, Beom J, Han TR, Oh B-M. Inter-rater agreement for the clinical dysphagia scale. *Ann Rehabil Med*. 2011;35(4):470.

67. Rost NS, Bottle A, Lee J, et al. Stroke Severity Is a crucial predictor of outcome: An international prospective validation study. *J Am Heart Assoc*. 2016;5(1):1-7.

68. Duan Y, Chen F, Lin L, Wei W, Huang Y. Leukoaraiosis rather than lacunes predict poor outcome and chest infection in acute ischemic stroke patients. *Int J Clin Exp Med*. 2015;8(10):19304-19310.

69. Kwee RM, Kwee TC. Virchow-Robin spaces at MR imaging. *Radiographics*. 2007;27(4):1071-1086.

70. Pantoni L, Basile AM, Pracucci G, et al. Impact of age-related cerebral white matter changes on the transition to disability -- the LADIS study: rationale, design and methodology. *Neuroepidemiology*. 2005;24(1-2):51-62.

71. Muñoz Maniega S, Chappell FM, Valdés Hernández MC, et al. Integrity of normal-appearing white matter: Influence of age, visible lesion burden and hypertension in patients with small-vessel disease. *J Cereb Blood Flow Metab*. 2017;37(2):644-656.

72. Lee WH, Chun C, Seo HG, Lee SH, Oh BM. STAMPS: Development and verification of swallowing kinematic analysis software. *Biomed Eng Online*. 2017;16(1):1-12.

73. Chan J, Gil H, Hyung W, Chan H. Computer-assisted detection of swallowing. *Comput Methods Programs Biomed*. 2016;134: 79-88.

74. Kendall KA, Leonard RJ. Hyoid movement during swallowing in older patients with dysphagia. *Arch Otolaryngol - Head Neck Surg*. 2001;127(10):1224-1229.

75. Levitin DJ, Nuzzo RL, Vines BW, Ramsay JO. Introduction to functional data analysis. *Can Psychol Can*. 2007;48(3):135-155.

76. Ramsay JO, Silverman BW. *Functional Data Analysis*. Second. New York: Springer-Verlag; 2005.

77. Chen T, Guestrin C. XGBoost: A scalable tree boosting system. *Proc ACM*

SIGKDD Int Conf Knowl Discov Data Min. 2016:785-794.

78. Natekin A, Knoll A. Gradient boosting machines, a tutorial. *Front Neurorobot*. 2013;7(21):1-21.

79. Liu L, Yu Y, Fei Z, et al. An interpretable boosting model to predict side effects of analgesics for osteoarthritis. *BMC Syst Biol*. 2018;12(Suppl 6).

80. He H, Bai Y, Garcia EA, Li S. ADASYN: Adaptive synthetic sampling approach for imbalanced learning. In: *2008 IEEE International Joint Conference on Neural Networks*. ; 2008:1322-1328.

81. He H, Garcia EA. Learning from imbalanced data. *IEEE Trans. Knowl. Data Eng.* 2009;21:1263–1284.

82. Santos MS, Soares JP, Abreu PH, Araujo H, Santos J. Cross-validation for imbalanced datasets: Avoiding overoptimistic and overfitting approaches. *IEEE Comput Intell Mag*. 2018;13(4):59-76.

83. Boughorbel S, Jarray F, El-Anbari M. Optimal classifier for imbalanced data using Matthews Correlation Coefficient metric. *PLoS One*. 2017;12(6):1-17.

84. Tantithamthavorn C, Hassan AE, Matsumoto K. The Impact of class rebalancing techniques on the performance and interpretation of defect prediction models. *IEEE Trans Softw Eng*. 2018:1-20.

85. Zou Q, Xie S, Lin Z, Wu M, Ju Y. Finding the best classification threshold in imbalanced classification. *Big Data Res*. 2016;5:2-8.

86. Paik NJ, Kim SJ, Lee HJ, Jeon JY, Lim JY, Han TR. Movement of the hyoid bone and the epiglottis during swallowing in patients with dysphagia from different etiologies. *J Electromyogr Kinesiol*. 2008;18(2):329-335.

87. Seo HG, Oh BM, Han TR. Swallowing kinematics and factors associated with laryngeal penetration and aspiration in stroke survivors with dysphagia. *Dysphagia*. 2016;31(2):160-168.

88. Park D, Lee HH, Lee ST, et al. Normal contractile algorithm of swallowing related muscles revealed by needle EMG and its comparison to videofluoroscopic swallowing study and high resolution manometry studies: A preliminary study. *J Electromyogr Kinesiol*. 2017;36:81-89.

89. Pearson WG, Langmore SE, Zumwalt AC. Evaluating the structural properties of suprahyoid muscles and their potential for moving the hyoid. *Dysphagia*. 2011;26(4):345-351.

90. Rassier DE, Macintosh BR, Herzog W. Length dependence of active force

production in skeletal muscle. *J Appl Physiol*. 1999;86(5):1445-1457.

91. Kim SM, McCulloch TM, Rim K. Comparison of viscoelastic properties of the pharyngeal tissue: Human and canine. *Dysphagia*. 1999;14(1):8-16.

92. Taylor DC, Dalton JD, Seaber A V., Garrett WE. Viscoelastic properties of muscle-tendon units: The biomechanical effects of stretching. *Am J Sports Med*. 1990;18(3):300-309.

93. Kang BS, Oh BM, Kim IS, Chung SG, Kim SJ, Han TR. Influence of aging on movement of the hyoid bone and epiglottis during normal swallowing: A motion analysis. *Gerontology*. 2010;56(5):474-482.

94. Hamdy S. Role of cerebral cortex in the control of swallowing. *GI Motil online*. 2006.

95. Hamdy S, Aziz Q, Rothwell JC, et al. Recovery of swallowing after dysphagic stroke relates to functional reorganization in the intact motor cortex. *Gastroenterology*. 1998;115(5):1104-1112.

96. Jang HJ, Leigh JH, Seo HG, Han TR, Oh BM. Effortful swallow enhances vertical hyolaryngeal movement and prolongs duration after maximal excursion. *J Oral Rehabil*. 2015;42(10):765-773.

97. Mann G, Hankey GJ, Cameron D. Swallowing function after stroke. *Stroke*. 2011;30(4):744-748.

98. Han TR, Paik NJ, Park JW, Kwon BS. The prediction of persistent dysphagia beyond six months after stroke. *Dysphagia*. 2008;23(1):59-64.

99. Milanlioglu A, Aydn MN, Gökgül A, Hamamc M, Erkuzu MA, Tombul T. Ischemic bilateral opercular syndrome. *Case Rep Med*. 2013;2013:3-6.

100. Bradley N, Hannon N, Lebus C, O'Brien E, Khadjooi K. Bilateral corona radiata infarcts: A new topographic location of Foix–Chavany–Marie syndrome. *Int J Stroke*. 2014;9(8):E39-E39.

101. Theys T, Van Cauter S, Kho KH, et al. Neural correlates of recovery from Foix-Chavany-Marie syndrome. *J Neurol*. 2013;260(2):415-420.

102. Van Tiggelen P, Danse E. Foix-Chavany-Marie or opercular syndrome. *J Belgian Soc Radiol*. 2015;98:56.

103. Yamanouchi H, Nagura H. Neurological signs and frontal white matter lesions in vascular parkinsonism. A clinicopathologic study. *Stroke*. 1997;28(5):965-969.

104. Jellinger KA. Vascular parkinsonism. *Therapy*. 2008;5(2):237-255.

105. Kwon HM, Lim. Risk of "silent stroke" in patients older than 60 years: risk assessment and clinical perspectives. *Clin Interv Aging*. 2010;5:239-251.

106. Kim BJ, Lee S-H. Prognostic impact of cerebral small vessel disease on stroke outcome. *J Stroke*. 2015;17(2):101.

107. Smith EE, Saposnik G, Biessels GJ, et al. Prevention of stroke in patients with silent cerebrovascular disease. *Stroke*. 2017;48(2):e44-e71.

108. Valdes G, Luna JM, Eaton E, Simone CB, Ungar LH, Solberg TD. MediBoost: A patient stratification tool for interpretable decision making in the era of precision medicine. *Sci Rep*. 2016;6(November):1-8.

109. Meyer S, Verheyden G, Brinkmann N, et al. Functional and motor outcome 5 years after stroke Is equivalent to outcome at 2 months: Follow-up of the collaborative evaluation of rehabilitation in stroke across Europe. *Stroke*. 2015;46(6):1613-1619.

110. Duncan PW, Sue Min Lai. Stroke recovery. *Top Stroke Rehabil*. 1997;4(3):51-58.

111. Wintzen AR, Badrising UA, Roos RA, Vielvoye J, Liauw L. Influence of bolus volume on hyoid movements in normal individuals and patients with Parkinson's disease. *Can J Neurol Sci*. 1994;21(1):57-59.

Supplemental Materials

Supplemental Table 1. Horizontal hyoid displacement (HD) and velocity (HV) in the backward motion that were associated with parameters of videofluoroscopic dysphagia scale in patients with Parkinson's disease (n=23)

	n	HD (mm)	*P*	HV (mm/%ile)	*P*
Triggering of pharyngeal swallow			0.181		0.292
Normal	19	-1.98±1.18		-0.22±0.11	
Delayed	4	-1.10±1.24		-0.14±0.15	
Vallecular residue			0.357		0.662
None	2	-3.05±0.91		-0.21±0.04	
<10%	13	-1.75±1.20		-0.23±0.14	
10-50%	5	-2.04±1.26		-0.19±0.08	
>50%	3	-1.02±1.18		-0.12±0.11	
Laryngeal elevation			0.881		0.025*
Normal	18	-1.84±1.15		-0.23±0.12	
Impaired	5	-1.80±1.57		-0.12±0.07	
Pyriform sinus residue			0.974		0.432
None	10	-1.82±1.15		-0.18±0.07	

<10%	10	-1.80±1.49		-0.21±0.17	
10-50%	2	-1.76±0.62		-0.26±0.04	
>50%	1	-2.34		-0.24	
Coating on the pharyngeal wall			0.867		0.462
No	7	-1.74±1.20		-0.17±0.06	
Yes	16	-1.87±1.26		-0.22±0.14	
Pharyngeal transit time			0.181		0.292
≤1.0 s	19	-1.98±1.18		-0.22±0.11	
>1.0 s	4	-1.10±1.24		-0.14±0.15	
Aspiration			0.675		0.486
None	3	-1.24±1.20		-0.15±0.11	
Supraglottic penetration	9	-2.02±1.32		-0.24±0.15	
Subglottic aspiration	11	-1.83±1.19		-0.18±0.09	

Values are presented as mean ± standard deviation.

*P-value<0.05.

Supplemental Table 2. Horizontal hyoid displacement (HD) and velocity (HV) in the forward motion that were associated with parameters of videofluoroscopic dysphagia scale in patients with Parkinson's disease (n=23)

	n	HD (mm)	*P*	HV (mm/%ile)	*P*
Triggering of pharyngeal swallow			0.224		0.123
Normal	19	9.18±3.04		0.67±0.28	
Delayed	4	7.71±2.80		0.45±0.14	
Vallecular residue			0.012*		0.041*
None	2	8.48±2.45		0.68±0.05	
<10%	13	10.62±2.73		0.73±0.30	
10-50%	5	6.74±1.19		0.51±0.12	
>50%	3	5.52±0.35		0.33±0.04	
Laryngeal elevation			0.157		0.602
Normal	18	9.34±2.75		0.63±0.25	
Impaired	5	7.44±3.69		0.61±0.38	
Pyriform sinus residue			0.224		0.187
None	10	10.06±3.00		0.75±0.30	

<10%	10	7.80±2.77		0.53±0.23	
10-50%	2	10.44±2.80		0.62±0.10	
>50%	1	5.88		0.36	
Coating on the pharyngeal wall			0.593		0.688
No	7	9.24±3.14		0.66±0.31	
Yes	16	8.79±3.02		0.61±0.26	
Pharyngeal transit time			0.224		0.123
≤1.0 s	19	9.18±3.04		0.67±0.28	
>1.0 s	4	7.71±2.80		0.45±0.14	
Aspiration			0.365		0.651
None	3	11.05±1.19		0.62±0.08	
Supraglottic penetration	9	9.03±3.27		0.70±0.32	
Subglottic aspiration	11	8.26±3.01		0.57±0.27	

Values are presented as mean ± standard deviation.

*P-value<0.05.

Supplemental Table 3. Vertical hyoid displacement (HD) and velocity (HV) in the forward motion that were associated with parameters of videofluoroscopic dysphagia scale in patients with Parkinson's disease (n=23)

	n	HD (mm)(mm)	*P*	HV (mm/%ile)	*P*
Triggering of pharyngeal swallow			0.035*		0.035*
Normal	19	12.49±5.20		0.76±0.16	
Delayed	4	7.66±2.05		0.49±0.19	
Vallecular residue			0.668		0.901
None	2	15.18±4.31		0.67±0.06	
<10%	13	11.41±5.90		0.72±0.20	
10-50%	5	10.19±2.62		0.70±0.17	
>50%	3	12.72±6.00		0.69±0.31	
Laryngeal elevation			0.709		0.180
Normal	18	11.83±5.32		0.74±0.19	
Impaired	5	11.00±4.78		0.61±0.18	
Pyriform sinus residue			0.440		0.228
None	10	11.04±4.87		0.67±0.16	
<10%	10	11.54±5.83		0.69±0.21	

10-50%	2	11.68±1.96		0.87±0.18	
>50%	1	18.64		1.00	
Coating on the pharyngeal wall			0.738		0.947
No	7	12.27±4.74		0.71±0.09	
Yes	16	11.37±5.40		0.71±0.23	
Pharyngeal transit time			0.035*		0.035*
≤1.0 s	19	12.49±5.20		0.76±0.16	
>1.0 s	4	7.66±2.05		0.49±0.19	
Aspiration			0.613		0.525
None	3	11.35±6.42		0.61±0.20	
Supraglottic penetration	9	10.03±3.22		0.69±0.12	
Subglottic aspiration	11	13.05±6.04		0.75±0.24	

Values are presented as mean ± standard deviation.

*P-value<0.05.

Appendix

국문 초록

뇌졸중과 파킨슨병 환자의 삼킴에 대한 운동학적 특징 분석 및 뇌졸중 후 삼킴곤란의 예후 예측 모델 개발

서울대학교 의과대학 의학과

의공학교실 이우형

서론: 삼킴곤란은 유병률이 증가하고 있는 뇌질환에서 가장 흔히 발생하는 증상 중 하나이다. 뇌질환 환자에서 삼킴곤란의 결과로서 발생할 수 있는 흡인성 폐렴이 사망의 중요 원인이 될 수 있기 때문에 삼킴곤란을 검사하고 관리하는 데에 특별한 관심이 필요하다. 본 연구의 목적은 파킨슨병과 뇌졸중 환자들의 삼킴에 대한 새로운 운동학적 특징을 탐색하고, 뇌졸중 후 삼킴곤란 환자들의 기능적 삼킴 상태를 예측하기 위한 머신러닝 기반의 예후 예측 모델을 개발하고 검증하는 것이다.

방법: 설골의 시공간적 데이터에 대한 운동학적 분석은 파킨슨병과 허혈성 뇌졸중 환자들을 대상으로 행하여졌다. 추가적으로 허혈성 뇌졸중 환자들은 6개월 후 삼킴 기능의 회복과 연관되어 있는 임상적, 영상학적 요인들을 탐색하여 운동학적 요인들과 함께 이용하여 6개월 후 삼킴 기능의 회복을 예측할 수 있는 예후 예측 모델을 개발하고자

하였다. 파킨슨병 환자군과 건강한 대조군에 대한 분석에서, 69명(23명의 파킨슨병 환자, 나이, 성별이 매칭된 23명의 건강한 노인 대조군, 23명의 건강한 젊은 대조군)의 연구대상자들의 비디오투시하 연하검사(VFSS) 영상으로부터 설골의 시공간적 데이터를 획득하였다. 삼킴 과정의 변위/속도의 정규화된 프로파일에 대하여 함수적 회귀 분석이, 그리고 이들의 최대값에 대한 비교 분석이 3개 그룹에 대하여 시행되었다. 뇌졸중 환자들의 운동학적 분석을 위하여 삼킴 평가를 위하여 VFSS가 의뢰된 137명의 일련의 허혈성 뇌졸중 환자들 중에서 18명의 나쁜 예후를 보이는 환자군(6개월 시점에 뇌졸중 이전의 상태로 회복되지 못한 경우)과 나이와 성별이 매칭된 18명의 좋은 예후를 보이는 환자군(6개월 시점에 뇌졸중 이전의 상태로 회복된 경우)이 선별되었다. 삼킴 과정의 변위/속도와 방향각의 정규화된 프로파일에 대하여 함수적 회귀 분석이, 그리고 이들의 최대값에 대한 비교 분석이 좋은 예후와 나쁜 예후 그룹에 대하여 시행되었다. 생존 분석에서 Kaplan-Meier 방법과 Cox 회귀분석 모델이 137명의 허혈성 뇌졸중 환자들에 대하여 삼킴 기능에 대한 나쁜 예후와 연관되어 있는 임상적, 영상학적 요인을 탐색하기 위하여 사용되었다. 관련된 운동학적, 임상적, 영상학적 요인들을 기반으로 삼킴 기능의 좋은 예후와 나쁜 예후를 가진 환자군을 분류하기 위한 익스트림 경사 부스팅(Extreme gradient boosting, XGBoost) 모델이 개발되었다. 개발된 모델은 5겹(5-fold) 교차 검증 방법으로 검증되었고 예측 성능은 서포트 벡터 머신, 랜덤 포레스트, 인공 신경망 등의 기준 머신 러닝에 기반을 둔 분류기들과 비교되었다.

결과: 파킨슨병과 건강한 대조군들에 대한 운동학적 분석에서 노인

대조군에 비하여 파킨슨병 환자군에서 설골의 최대 수평 변위 및 속도가 초기 역방향(P=0.006, P<0.001)과 정방향(P=0.008, P<0.001) 운동에서 유의하게 감소하였다. 최대 수직 속도는 파킨슨병 환자군에서 노인 대조군에 비하여 유의하게 감소하였다(P=0.001). 노인 대조군과 젊은 대조군 사이에 수평과 수직 방향의 최대 변위와 속도 모두 유의한 차이는 관찰되지 않았다. 허혈성 뇌졸중 환자들에 대한 운동학적 분석에서 설골의 최대 수평 변위(P=0.031) 및 속도(P=0.034)는 정방향 운동에서 좋은 예후와 나쁜 예후 환자 사이에 유의한 차이를 보였다. 삼킴 초기의 평균 방향각은 두 그룹 사이에 유의한 차이가 관찰되었다. 뇌졸중 후 삼킴곤란 환자들에 대한 생존 분석에서 24(17.5%)명의 환자에서 6개월까지 삼킴곤란의 지속이 관찰되었으며 평균 기간은 65.6일이었다. 뇌졸중 후 삼킴곤란의 기간은 초기 VFSS에서의 경관식이, 삼킴곤란 임상척도(clinical dysphagia scale, CDS), 성별, 중증 뇌백질 고신호병변(white matter hyperintensities, WMH), 양측의 방사관/기저핵/내섬유막의 손상에 의해서 유의한 차이가 관찰되었다. 이 요인들 중 초기 VFSS에서의 경관식이(P<0.001), 양측의 방사관/기저핵/내섬유막의 손상(P=0.001), 삼킴곤란 임상척도(P=0.042)가 Cox 회귀모델의 다변량 분석에서 유의한 예측 인자로 관찰되었다. 6개월째 삼킴 회복의 예측에서 XGBoost 분류기는 AUC 0.881, F1 점수 0.945, 매튜 상관 계수 0.718을 보이며 서포트 벡터 머신, 랜덤 프레스트, 인공 신경망 등의 다른 기준 알고리즘에 근거한 분류기들보다 우월한 성능을 보였다.

결론: 본 연구는 삼킴 과정의 설골의 초기 역방향 운동의 이상이 삼킴곤란이 있는 파킨슨병 환자들과 허혈성 뇌졸중 환자들이 보이는

새로운 운동학적 특징이 될 수 있음을 보였다. 허혈성 뇌졸중 환자들에서 초기 삼킴곤란의 심각도와 양측의 방사관/기저핵/내섬유막의 손상이 6개월째 삼킴 기능의 회복과 유의하게 연관되어 있는 임상적, 영상학적 요인들이었다. 제안된 XGBoost 모델이 운동학적, 임상적, 영상학적 요인들에 근거하여 뇌졸중 후 6개월째 삼킴 회복을 예측하는 것이 가능하였음을 보였다. 본 연구는 설골의 초기 역방향 운동의 이상과 양측의 피질하 영역의 손상이 허혈성 뇌졸중에서 장기간의 삼킴 회복을 위한 예후 예측 모델을 개발하는데 중요한 예후 인자임을 강조한다. 추후 연구로서 초기 설골의 움직임과 양측 피질하 영역의 손상의 삼킴 기능에 대하여 생리학적 측면에서 탐색하고, 이러한 연구 결과들에 근거를 둔 장기 삼킴 회복에 대한 예후 예측 모델의 개선이 필요하다.

주요어: 뇌졸중, 동작 분석, 머신러닝, 삼킴, 생존 분석, 설골, 예후, 파킨슨병, 함수적 데이터

학번: 2012-23642